Title
Ciliary signaling in oligodendroglial development and white matter injury repair

Permalink
https://escholarship.org/uc/item/4gt320wm

Author
Hoi, Kimberly Kam

Publication Date
2023

Peer reviewed|Thesis/dissertation

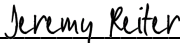Ciliary signaling in oligodendroglial development and white matter injury repair

by
Kimberly Kam Hoi

DISSERTATION
Submitted in partial satisfaction of the requirements for degree of
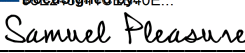DOCTOR OF PHILOSOPHY

in

Biomedical Sciences

in the

GRADUATE DIVISION
of the
UNIVERSITY OF CALIFORNIA, SAN FRANCISCO

Approved:

Jeremy Reiter
_____
Chair

Stephen Fancy
_____

Samuel Pleasure
_____

_____

_____
Committee Members

For

My grandparents,

Ut Heong Chio and Keng Fan Hoi

&

My parents,

Maings Hoi and Sharon Chao

Acknowledgements

The work presented in this dissertation shows only a piece of my journey to earning a PhD. What it doesn't show is that this period of my life was one of tremendous scientific and personal growth, supported by many individuals who generously shared their time with me and to whom I must express my gratitude. First, I would like to thank my thesis advisor, Steve Fancy, for his steadfast support through all the trials and tribulations of my graduate school experience. His guidance and scientific mentorship have significantly influenced how I approach new scientific questions and challenges. He allowed me to freely explore my scientific interests and provided me with opportunities to exercise my independence while helping me refocus when needed. My time in his lab has taught me to be more confident in myself and to celebrate my achievements; for all of this, I am grateful. I also want to thank the members of Steve's lab, past and present, for answering all my questions, teaching me what they know, and inspiring me to continuously strive to become a better person and scientist.

Outside of Steve's lab, the scientific environment at UCSF offered opportunities for collaboration and discussion with friendly and extremely intelligent people. My thesis committee members Jeremy Reiter and Samuel Pleasure were always willing to extend advice and feedback as I navigated my research project. I am thankful to Jeremy for answering all our cilia-related questions and providing valuable insights that drove this project forward. I am thankful to Sam for his ideas on central nervous system development and for reviewing my data with a critical eye. Their encouragement and support through this process helped me reach the end. In addition to my thesis committee, I am grateful for collaborations with Maxence Nachury and Ruth Huttenhain. Maxence's perspectives on the composition of cilia and Ruth's mass spectrometry expertise form some of the exciting new directions that can be taken from the work presented in this dissertation. I would also like to acknowledge Jonah Chan for the career mentorship and scientific advice he gave me throughout the years.

Contributions

The work in this dissertation was performed in the laboratory of Dr. Stephen P.J. Fancy at the University of California, San Francisco. Thesis committee chair Dr. Jeremy F. Reiter and committee member Dr. Samuel J. Pleasure provided valuable insights to the project. I wrote this dissertation with the following contributions.

Chapter 2 is adapted from the following manuscript that is in submission:

Hoi, K.K., Xia, W., Wei, M.M., Ulloa-Navas, M.J., Garcia-Verdugo, J.M., Nachury, M.V., Reiter, J.F., and Fancy, S.P.J. Primary cilia control OPC proliferation in white matter injury via Hedgehog-independent CREB signaling.

K.K.H and S.P.J.F conceived and designed all experiments. K.K.H performed experiments and analyzed data. W.X. and M.M.W contributed to sample preparation, and M.J.U.N and J.G.M.V contributed to electron microscopic analysis of cilia. J.F.R contributed to analysis of RNA-sequencing data. M.V.N. and J.F.R. contributed to discussion. K.K.H and S.P.J.F wrote and edited the submitted research manuscript. S.P.J.F. was supported by grants from NIH/NINDS (R01NS128021, P01NS083513, R21NS133891). S.P.J.F. is a Harry Weaver Neuroscience Scholar of the National Multiple Sclerosis Society.

Chapter 3 contains preliminary work that has not been published. Maxence Nachury developed the method, and Ruth Huttenhain performed the LC-MS-MS and analysis. I performed the remaining experiments.

Ciliary signaling in oligodendroglial development and white matter injury repair

Kimberly Kam Hoi

Abstract

After damage to white matter tracts in central nervous system (CNS) diseases such as multiple sclerosis (MS), myelin sheaths can be regenerated by activated oligodendrocyte precursor cells (OPCs). Failure of this remyelination program often occurs due to the improper expansion of the OPC population within sites of injury, contributing significantly to ongoing neurological dysfunction and disease progression. Understanding the biological underpinnings of developmental myelination and remyelination will reveal novel therapeutic strategies for disorders involving dysfunctional myelin regeneration. Importantly, OPCs dynamically produce primary cilia, microtubule-based organelles that transduce cues in a specialized signaling compartment. Here, we show that OPCs require primary cilia to respond properly to white matter injury (WMI). We demonstrate that removing primary cilia from OPCs results in significantly reduced OPC proliferation during both CNS development and WMI repair. Furthermore, we uncover a role for cAMP and CREB-mediated transcription, but not Hedgehog (Hh) signaling, in the ciliary control of OPC proliferation. This leads us to propose a G-protein coupled receptor (GPCR)/cAMP/CREB signaling axis initiated at the primary cilium as a crucial regulator of OPC biology. These findings advance our understanding of how OPCs coordinate complex cellular cues during remyelination in the CNS and presents the primary cilium as an organelle from which novel targets for remyelinating therapies may be identified.

Table of Contents

List of Figures

List of Tables

Chapter 1: Introduction

Multiple sclerosis

      In 2020, there were an estimated 2.8 million people with multiple sclerosis (MS) worldwide, 1 million of which live in the United States (National Multiple Sclerosis Society)[1]. Multiple sclerosis is an autoimmune disease wherein the body's immune system attacks central nervous system (CNS) myelin, which is produced by oligodendrocytes (OLs)[2]. Pathology includes axonal damage, demyelination, and often gliosis. MS presents early in adult life and can impair vision, movement, muscle strength, coordination, and cognition. In addition to these functional consequences, MS greatly reduces the quality of life and presents a heavy financial burden to patients[3].

      The International Advisory Committee on Clinical Trials of MS divided the disease into four disease courses: clinically isolated syndrome (CIS), relapsing-remitting MS (RRMS), primary progressive MS (PPMS), and secondary progressive MS (SPMS)[4]. CIS usually describes the first episodes of symptoms caused by CNS inflammation and demyelination that are like those found in MS but may not necessarily progress into MS. Most patients with MS are diagnosed with RRMS, which consists of a pattern of new or worsening neurologic symptoms defined as "attacks" or "relapses" followed by periods of recovery known as "remission." While 85% of patients are first diagnosed with RRMS, this disease course can progress to SPMS. SPMS is defined by worsening or accumulating neurologic function over time. Lastly, patients diagnosed with PPMS exhibit worsening neurologic dysfunction at symptom onset[5].

      Many disease-modifying therapies (DMT) now exist for RRMS and have been shown to increase lifespan and improve neurologic function. Positive outcomes of existing treatments include the decrease in rate of RRMS progressing to SPMS compared to historical data, based on clinical and MRI data of MS patients actively undergoing treatment[6]. Additionally, a longitudinal study examining the survival and cause of death in a 60-year population-based MS cohort compared to the general population shows that mortality has improved. Still, MS patients exhibit a shorter life expectancy and threefold higher mortality compared to the general population. The disease burden of MS also involves symptoms that significantly reduce the quality of life of

patients, highlighting the importance of improving the existing MS treatments to ameliorate symptoms and combat progressing neurologic decline[7].

Strategies for treating multiple sclerosis

The DMTs that are currently available for MS often target inflammation, with very few drugs in the pipeline to address accumulated tissue damage contributing to neurologic dysfunction. The Interferon β (IFNβ) class of medications are immunomodulators that reduce antigen presentation, decrease T helper cell cytokine expression, and increase production of anti-inflammatory cytokines[8]. Licensed IFNβ drugs include Avonex (IFNβ1a), Rebif (IFNβ1a), Betaferon (IFNβ1b), and Extravia (IFNβ1b). The attachment of polyethylene glycol to IFN has been shown to extend the time of biological effect of IFN, therefore pegylated IFNβ1a, Plegridy, has also been used to treat MS. Other approved drugs that dampen unfavorable immune responses while inducing anti-inflammatory immune profiles include: Copaxone (glatiramer acetate), Tecfidera (dimethyl fumarate), Aubagio (teriflunomide), and Gilenya (sphingosine 1 phosphate receptor antagonist)[3].

More recently, monoclonal antibodies (mAbs) have been used to treat MS. These mAbs tend to be more specific than other drug modalities and have fewer off-target effects, especially with the application of humanized mAbs[9]. While many mAbs have been tested in clinical trials, such as rituximab, only three humanized mAb therapies are currently approved for treatment of MS. Tysabri (natalizumab) behaves as an α4 integrin blocker that effectively prevents the invasion of lymphocytes through the blood-brain barrier into the CNS. Lemtrada (alemtuzumab) targets the surface antigen CD52 on lymphocytes and monocytes, resulting in T and B cell depletion. Finally, Ocrevus (ocrelizumab) is a B cell-depleting mAb that targets CD20[3]. While each of these humanized mAbs is approved for the treatment of CIS, RRMS, and active SPMS, only ocrelizumab has FDA approval for the treatment of PPMS. This is because there is data to support that ocrelizumab slows PPMS progression as indicated by clinical and MRI data of MS patients treated with ocrelizumab compared to placebo[10]. Therefore, while the development and

optimization of mAbs for MS treatment is promising, the approved drugs are only partially effective as MS therapies. A more comprehensive approach to MS treatment would involve the generation of reparative drugs to address lost axons and myelin.

Promoting remyelination

There is currently an absence of drugs that promote the repair of CNS damage from MS to prevent the progressive accumulation of neurological disability[11]. One component of tissue repair is remyelination, a process that involves the regeneration of myelin in areas that have been demyelinated to restore the efficacy of saltatory conduction and support axonal health. In the CNS, new myelin is generated by OLs. One way that this can occur is through the activation of oligodendrocyte precursor cells (OPCs) that divide, migrate to demyelinated regions, and differentiate into newly generated OLs that eventually form myelin[12]. Historically, this was the model in which new myelin was believed to be generated. However, recent evidence suggests that remyelination can occur from old, existing OLs that extend processes from their surviving cell bodies to generate new myelin[13]. After demyelination, surviving OLs have displayed a tendency to mistarget – for instance, to the cell bodies of neurons – suggesting that remyelination is more efficient and precise from newly generated OLs[14]. Identifying ways to promote remyelination could improve neurologic function in MS, a disease in which demyelination is a central component.

Remyelination in white matter injury (WMI), and especially in MS, often fails. Evidence suggests that this is due to the inefficient differentiation of OPCs into OLs within demyelinated lesions. Therefore, studies focus on identifying mechanisms within OPCs that can be targeted to promote their differentiation in disease and injury. These strategies include developing antibodies targeting inhibitors of differentiation and performing drug screens for compounds that directly enhance differentiation. In 2014, a study using micropillar arrays for a high-throughput screen of a compound library identified a cluster of anti-muscarinic compounds that enhanced OL myelination. Importantly, the authors showed that clemastine, a widely available antihistamine

traditionally used for the treatment of allergies, exhibits anti-muscarinic properties that promote OPC differentiation and myelination of micropillars[15]. This is supported by further experiments showing that treatment with clemastine enhances OPC differentiation, myelination, and functional recovery in a neonatal hypoxia mouse model of WMI[16]. An additional screen of molecules targeting G-protein coupled receptors (GPCR) using micropillars showed that kappa-opioid receptor (KOR) agonists significantly increase oligodendroglial differentiation and myelination, identifying KOR as a relevant therapeutic target for remyelination[17].

While therapies for remyelination have focused on promoting OPC differentiation, other mechanisms of OPC biology fail during remyelination that deserve equal attention. Analysis of chronically demyelinated lesions indicates that OPCs are depleted in lesions and that OPCs fail to migrate to lesions[18, 19]. This suggests that promoting remyelination not only entails overcoming a differentiation block, but also promoting OPC migration and intralesional proliferation. Understanding the basic mechanisms underlying these processes during development can provide valuable insights into therapies for myelin regeneration that can be used in conjunction with the previously approved therapies that target the immune component of MS.

Oligodendrocyte development

The regenerative process of remyelination often recapitulates mechanisms that govern OL biology during development. In the developing mouse, OPCs first appear in the CNS at around embryonic day E12.5 (E12.5) near the ventral floor plate of the spinal cord at the pMN[20]. After their specification from the ventricular zones of the brain and spinal cord, OPCs migrate and proliferate to populate the entire CNS. These cells then decide whether to differentiate into an OL that generates myelin or to remain a progenitor. OPCs that remain progenitors comprise 5% of the cells in the adult CNS, and retain their abilities to divide, migrate, and differentiate to generate new myelin in the CNS in response to injury and neuronal activity[21]. In the following sections, I

provide an overview of what we know about the mechanisms regulating these distinct stages of OPC biology, with a focus on extrinsic factors.

OPC specification

In the developing mouse, OPCs emerge from the ventral spinal cord pMN domain around E12.5 in a process that mirrors motor neuron (MN) generation from the same domain at E9.5[22]. A second wave of OPCs then emerges from the dorsal spinal cord around E15.5[23-25]. These dorsally derived OPCs comprise 20% of the OPCs in the mouse spinal cord while the remaining 80% originate from the ventral spinal cord. In the developing forebrain, OPC specification also occurs in distinct waves following a ventral to dorsal pattern of emergence. OPCs first emerge from the ventricular zone (VZ) of the medial ganglionic eminence (MGE) at around E12.5 from Nkx2.1 expressing progenitors in a Shh-dependent manner. This is followed by a second wave of OPCs that derive from Gsx2-expressing progenitors in lateral ganglionic eminence (LGE) at E15.5. From the GEs, OPCs migrate dorsally and laterally to occupy the rest of the brain and cortex. A final wave of OPCs then emerges early postnatally from the Emx1-expressing progenitors of the cortical VZ. Lineage tracing analyses from the VZ progenitors driving this specification indicate that after birth, 80% of the remaining OPCs are Emx1-derived, with a 20% contribution from the LGE Gsx2 expressing progenitors, a contrast to the contributions of OPCs derived from dorsal and ventral origins in the spinal cord[26].

The specification of OPCs from neural progenitors is mediated by diffusible signals that exist in a gradient around the ventricular zone of the spinal cord, including Shh from the floor plate and Wnt/BMP from the roof plate. The gradient of Shh expression in the spinal cord results in the activation of different sets of transcription factors that regulate cell fate determination from VZ neural progenitors[27]. At the pMN, Shh acts through its effector Gli1 to promote the critical expression of the basic-helix-loop-helix (bHLH) transcription factor Olig2, which is required for both MN and OPC generation[21]. During MN generation, Olig2 is phosphorylated at Ser147, driving

the formation of homodimers. Dephosphorylation of Olig2 triggers a preferential formation of heterodimers with Neurogenin 2 or other bHLH proteins, resulting in a switch from MN to OPC production[28]. Knockout studies show that Shh is required for the specification of the ventral source of OPCs in mice, but not those emerging from the dorsal spinal cord[29, 30]. As opposed to this, Shh seems to be involved in the specification from all sources of OPCs in the forebrain, where Shh is expressed by precursors located at the MGE and LGE beginning at E10.5, resulting in *Olig2* expression[31, 32]. The dorsal Emx1 derived OPCs of the cortex also require Shh signaling for specification. Deletion of Shh from interneuron sources results in a significant reduction of OLs in the cortex while knockout of the Shh antagonist Sufu increases OL production in the neocortex[33].

More recent studies suggest that OPC specification is regulated by crosstalk between neural progenitors and endothelial cells. Ang-1 expression in neural progenitors, which is driven by Shh, signals to endothelial cells expressing Tie2. Tie2 then stimulates the production of TGFβ that then instructs neural progenitors to commit to their OPC fate[34]. The involvement of this crosstalk in OPC specification is interesting given that similar interactions with endothelial cells appear later when OPCs migrate throughout the brain and spinal cord on blood vessels[35, 36].

Critical mechanisms shaping oligodendrocyte development and CNS myelination

Once generated from the VZ of the developing mouse embryo, OPCs are instructed to migrate and proliferate in response to an ensemble of factors. Immediately upon specification, OPCs are characterized by their expression of platelet derived growth factor receptor (Pdgfrα). Pdgf-AA, secreted by neurons and astrocytes, acts on OPC Pdgfrα to promote the survival and proliferation of OPCs[37-42]. In the absence of Pdgf-A, OPCs are depleted in the CNS and mice exhibit hypomyelination[37]. Conversely, overexpressing Pdgf-A in astrocytes promotes OPC proliferation, resulting in an observed increase in the number of OPCs populating the developing CNS and areas of demyelination in lysolecithin and cuprizone models of WMI[43]. Therefore, PDGF signaling in OPCs plays a critical role in the maintenance and activation of OPCs throughout the

7

mouse CNS. Other polypeptide growth factors have been implicated in promoting OPC proliferation. For instance, OPCs express Fgf receptors (Fgfr) and proliferate in response to Fgf ligands *in vitro*. However, it is unclear whether this is relevant *in vivo*, as genetic knockouts of different Fgfrs in mice indicate that OPC proliferation does not require Fgf signals[21].

In the spinal cord, the initial dispersion of OPCs from the VZ is mediated by netrin-1. In netrin-1 mutants, OPCs are unable to migrate away from the VZ and instead accumulate around the ventral spinal cord[44]. After dispersal from the germinal zones, OPCs migrate along blood vessels in the developing CNS, using them as a substrate on which they crawl or jump, from one vessel to another, to their target destination[35]. This attachment is mediated by Wnt-induced OPC expression of Cxcr4 which binds to endothelial Sdf1 (Cxcl12). Since Wnt signaling has been previously implicated to block OPC differentiation, the Wnt-dependent OPC-endothelial interaction works to keep OPCs as migrating progenitors while inhibiting their ability to differentiate. Detachment of OPCs from their migratory scaffold once they are positioned correctly is therefore necessary for their subsequent differentiation. Indeed, once OPCs are displaced from blood vessels by astrocyte endfeet via a Sema3a/6a repulsion mechanism, they are shielded from this maturation inhibitory endothelial niche and differentiate[45].

In addition to mediating the association between OPCs and the vasculature during developmental migration, the Wnt pathway is a critical regulator of OL maturation. Evidence supports a mechanism in which increased Wnt pathway activation inhibits the differentiation of OPCs into OLs. Developmental myelination and remyelination are delayed in mice when Wnt signaling is constitutively active in OL lineage cells that express dominant-active (DA) β-catenin[46]. Furthermore, Wnt inhibitor XAV939 stabilization of Axin2, a Wnt target that participates in negative feedback regulation of the pathway, accelerates differentiation and myelination/remyelination after hypoxic and focal demyelinating injuries[47]. While these studies exemplify that canonical Wnt signaling in OPCs prevents OL maturation, a role for Wnt signaling in promoting processes required for OL differentiation and myelination has also been reported. Wnt3a overexpression in

the subependymal zone (SEZ) of adult mice increases the production of OPCs that could be reversed through β-catenin inhibition[48]. Tcf7l2/Tcf4 expression is significantly reduced in hypomyelination models, and expression of mature OL markers Plp and MBP is reduced when Tcf4 is deleted, resulting in deficient myelin repair after injury[49]. These seemingly contradictory findings could be a result of the Wnt signaling pathway exerting distinct effects on OLs as they progress through different stages of development or the fine-tuning of Wnt tone in these cells.

After OPCs differentiate into OLs, these mature OLs can generate myelin internodes adjacent to nodes of Ranvier[50] on multiple axons. Myelin ultimately provides metabolic support and allows for the rapid conduction of action potentials across these axons in the CNS[51]. While the majority of myelination occurs during postnatal development, a stable pool of OPCs that persists in the adult can generate OLs that produce myelin throughout life. *In vitro,* OLs can myelinate nanofibers above a threshold diameter (>0.4 μm), demonstrating the intrinsic capacity for OLs to myelinate objects of the correct size[52]. Interactions with cues in the environment also instruct myelination, including cell-to-cell interactions with microglia, astrocytes, and neurons[53]. Recent studies look at experiences such as motor learning[13, 54], socialization[55], sensory stimulation[50], stress[56], and fear[57] that can all contribute to new myelin formation.

Overall, myelination is a well-orchestrated program that involves OPC migration, maturation, and OL myelination of target axons. Each of these cellular processes require intrinsic and extrinsic cues. What has been described so far is in no way a comprehensive review of every signal regulating OL biology, and an overwhelming number of signals – including diffusible proteins, contact/adhesion-based signals, and neuronal activity – are involved in ensuring proper myelination of the CNS. How does an OPC keep track of when, where, and how to respond to all these environmental cues? The most basic answer to this question is that OPCs synchronize the expression of the appropriate surface proteins and receptors alongside their intracellular pathway effectors, in proximity, at the correct place and time. This would allow for the efficient spatial modulation of signaling initiation, kinetics, and output. A quintessential example of such signaling

compartmentalization in vertebrate cells is the signaling organelle known as the primary cilium. The role of signaling through primary cilia in OPC biology is the subject of this dissertation.

Primary cilia

The primary cilium is a cellular organelle that presents as a hair-like protrusion from the plasma membrane of most vertebrate cell types. They extend as a solitary non-motile unit on each cell, which differs from the secondary, motile cilia that are often present on cells in large numbers (i.e., ependymal cell cilia that push CSF through central nervous system ventricles)[58]. Primary cilia are primarily sensory organelles that are enriched in receptors to transduce extracellular cues that mediate a diverse set of cellular processes including proliferation, migration, differentiation, and cell survival[59]. Due to their crucial roles in these developmental processes, mutations that disrupt the ciliary machinery or ciliogenesis can result in disorders known as ciliopathies, which can affect most vertebrate tissue systems[60].

The core structure of the primary cilium is a microtubule-based axoneme, where microtubules are arranged in a ring of nine doublets (9+0 arrangement)[61]. This is anchored to a modified centriole known as the basal body[62]. Fibers in the transition zone dock the basal body to the plasma membrane and create a diffusion barrier to tightly regulate the entry and exit of proteins into and out of the primary cilium[59]. Selected proteins, which may require special ciliary targeting sequences (CTS), are transported up and down the cilium via a conserved mechanism of intraflagellar transport (IFT), which was discovered in the flagella of *Chlamydomonas reinhardtii*[63]. Two major IFT complexes contribute to ciliary cargo transport: IFT-A and IFT-B. The IFT-B complex carries cargo from the base to the tip of the cilium (anterograde) using kinesin-2 motor proteins while IFT-A particles are involved in transport from the tip back to the base of the cilium (retrograde) using a dynein motor[64, 65].

IFT contributes not only to the transport of proteins involved in supporting the structure of cilia, but also those required for signaling pathways mediated by primary cilia in cells. These

signaling components, including receptors and their pathway effectors, can be activated at the cilium to achieve effects that are distinct from those instructed when activation occurs in the cytoplasm[66], exemplifying how specific signaling can be depending on where a signal is activated. Crucial receptors and effectors of Hedgehog (Hh) and GPCR signal transduction localize to vertebrate cilia[67-69].

Hedgehog signaling in the primary cilium

The Hedgehog signaling pathway regulates a multitude of cellular processes important for the development of every organ in the body, ranging from tissue patterning and organogenesis to maintaining cellular homeostasis[70]. In the OL lineage, Hh is required for the proper specification of OPCs in the developing mouse CNS[71]. Generally, phenotypes associated with ciliary mutations are often the same as those arising from dysregulated Hh signaling in vertebrates. This link was first established in a forward genetic screen in mice, when defects in IFT were shown to affect Hh signaling[72]. It is now widely accepted that vertebrate Hh signaling requires primary cilia for amplification of pathway activation. Consistent with this, Hh pathway components Patched-1 (Ptch1), Smoothened (Smo), and Gpr161 localize to cilia[67, 68, 73].

The transcriptional effectors of the Hh pathway are Gli proteins. These proteins exist as activators (GliA) or repressors (GliR) to positively regulate or basally repress pathway activation[74]. Activation of the Hh pathway occurs when Hh ligand binds to its receptor, Ptch1, triggering Ptch1 clearance from the cilium via endocytosis. Consequently, GPCR-like Smo, a seven-transmembrane receptor, accumulates in the cilium resulting in the downstream activation of Gli effectors (GliA) and the transcription of Hh target genes[67]. Smo translocation to the cilium also triggers Gpr161 exit to derepress Hh. Gpr161, a $G\alpha_s$-coupled receptor, antagonizes Hh signaling via its ciliary accumulation. In the absence of Hh ligand, Gli transcriptional effectors are proteolytically processed into their repressor forms (GliR) to suppress Hh pathway activation.

During this time, Gpr161 localizes at the cilium and couples to Gαs. This negatively regulates Hh signal transduction by maintaining high cAMP and PKA activity[68].

GPCR enrichment in the primary cilium

G-protein coupled receptors represent the largest class of signaling receptors and display impressive functional diversity. This class of receptors is defined by a shared structure comprising an extracellular N-terminus, seven transmembrane domains (7-TM), and an intracellular C-terminus[75]. At the plasma membrane, ligand binding to GPCR causes a conformational change that activates GTP-binding proteins (G-proteins), which consist of α, β, and γ subunits. The function of the G-protein depends on the associated α-subunit, which can be categorized into $G\alpha_s$, $G\alpha_i$, $G\alpha_o$, or $G\alpha_{12}$. $G\alpha_s$-coupled proteins tend to be stimulatory on adenylyl cyclases to produce cAMP, while $G\alpha_{i/o}$ inhibit adenylyl cyclase and cAMP production. Agonist binding leads to GDP release and GTP-binding of α-subunits, with subsequent involvement of intracellular effectors that regulate downstream signaling[69, 76].

Several GPCRs and their pathway effectors have now been localized to cilia, suggesting that primary cilia can accomplish their diverse effects by acting as GPCR signaling centers. In addition to GPCRs that modulate Hh signaling in the cilium, like Gpr161, numerous other GPCRs localize to cilia. In the CNS, several GPCRs are selectively enriched in neuronal cilia. The neurotransmitter somatostatin is an important regulator of cognitive function, and its receptor, somatostatin receptor subtype 3 (SSTR3) localizes in cilia[77]. Loss of SSTR3 or cilia in the hippocampus results in memory deficits[78]. The melanocortin 4 receptor (MC4R), which functions in energy regulation, also localizes to neuronal cilia and deletion of the cilium results in dysregulated energy homeostasis associated with loss of MC4R[79, 80]. Other GPCRs with confirmed ciliary localization in the CNS include NPY2R, NPY5R[81], KISS1R[82], MCHR1[83], 5-HTR$_6$[84], and QRFPR[81] in neurons and PRLHR[85] in glia. As more GPCRs are added to the list of ciliary-localized GPCRs, it will be interesting to determine whether cilia-specific localization in

distinct cell types specifies the signaling output of these receptors compared to their counterparts in the plasma membrane.

Primary cilia in oligodendroglial lineage cells

In the mouse CNS, granule cell precursors of the EGL[86, 87], the V-SVZ[88] and SGZ neural stem cells [89, 90], astrocytes, neurons[58, 79, 80, 91], and OPCs[92-94] harbor primary cilia. OPCs purified from the differential shaking of mixed glial cultures of rat cortices were shown to present cilia labeled with acetylated tubulin in the vicinity of γ-tubulin labeled basal bodies. In these cultures, primary cilia are undetectable in MBP$^+$ OLs. These OPCs displayed a severely damaged and unbranched phenotype upon disruption of the primary cilium using ciliobrevin, a dynein inhibitor that prevents retrograde transport in cilia. OPCs were rescued from this damage when cultured in the presence of Shh[92]. This study would suggest that OPCs require primary cilia for survival and process extension. However, as ciliobrevin is not a cilium-specific dynein inhibitor, an alternative interpretation of the data would be that the phenotype is arising from off-target effects on cytoplasmic dynein. A more specific approach to disrupting ciliogenesis would confirm whether OPCs require primary cilia for survival.

A more recent study disrupted ciliogenesis by deleting kinesin family member 3a (Kif3a), a critical gene for anterograde transport within the primary cilium. Kif3a, along with Kif3b and Kap3, is a subunit of Kinesin-II. Conditional deletion of Kif3a from OPCs in adult mice *in vivo* results in reduced OPC proliferation and oligodendrogenesis in the adult corpus callosum and motor cortex. This reduction contributes to an observed motor impairment phenotype on a treadmill assay, where loss of Kif3a in the OPC primary cilium leads to shorter stride length and increased stride frequency stemming from forelimb gait dysfunction[93]. These studies suggest a functional role for primary cilia on OPCs, but the extent to which the primary cilium contributes to signaling in an OPC is poorly understood. Specifically, the specific signaling pathways regulated by the primary cilium in OPCs have not previously been studied. Given the importance of the

primary cilium in transducing Hh and GPCR signals, whether OPCs transduce Hh through the cilium and if specific GPCRs localize to OPC primary cilia are important areas for future investigation. Both Hh and several GPCRs have been studied previously in OPC biology.

Hedgehog signaling in the oligodendrocyte lineage

The specification of OPCs from neural progenitors requires Hh signaling. However, a role for Hh signals in OPCs and OLs after they are generated remains unclear. Treatment of OPCs from mixed glial cultures with cyclopamine, a Hh inhibitor, results in decreased differentiation of OLs that is reversed upon co-treatment with Smoothened agonist (SAG)[95], indicating that Hh might be required for OL differentiation. However, one study suggests that OPCs may not require Hh for proper OL development at all. Hyperactivation of Smo to promote Hh signaling in neural progenitors using Nestin-Cre leads to the ectopic induction of OL lineage cells, confirming the requirement for Hh in OL lineage specification. On the other hand, deletion of Smo specifically from OPCs after their specification produces no observable deficits in OPC distribution or development, suggesting that Hh signaling and Smo are not required for OL development. Interestingly, overexpression of Smo specifically in OPCs after specification promotes OPC proliferation while inhibiting OL differentiation[96]. This is consistent with another study showing that injection of Shh into lateral ventricles increases the numbers of proliferating OPCs in the adult mouse brain[97]. Together, these studies indicate that OPCs and OLs can be receptive to Hh signals during development but may not normally activate this pathway to achieve their cellular processes, at least not under homeostatic conditions.

In the mouse model of corpus callosum demyelination induced by lysolecithin, OL lineage cells within white matter lesions display increased expression levels of Shh transcripts and protein which corresponds with an increase in Hh target genes in OL lineage cells compared to controls. Adenoviral transfer of recombinant Shh to the lesioned brain reduces lesion area while increasing the densities of OPCs and OLs in the lesion, effects which are attributed to Hh signals instructing

OPC survival, proliferation, and differentiation. Blocking Shh in lesions with Hh interacting protein (HHIP) prevents repair by disrupting OPC proliferation and differentiation[98]. Therefore, Hh signaling, although not required for OL development, might be reactivated during injury to promote remyelination. Whether these Hh signals are transduced through the primary cilium in OPCs remains unstudied.

GPCRs in the oligodendrocyte lineage

Several GPCRs have now been identified that regulate different stages of OL development, with activation of these different GPCRs engaging distinct downstream intracellular effectors. Gpr56 is an adhesion GPCR that is highly expressed in OPCs but not OLs during mouse development[99]. Parallel studies impairing Gpr56 function in zebrafish or removing Gpr56 from mice display a hypomyelination phenotype, with this deficit being caused by decreased OPC proliferation and generation of OLs[100, 101]. This occurs through Gpr56 interaction with $G\alpha_{12/13}$ and RhoA; Gpr56 mutants display decreased RhoA expression[101] while overexpression of RhoA rescues the hypomyelination observed in Gpr56 mutant zebrafish[100]. This exemplifies a role for the adhesion Gpr56 in facilitating intracellular signaling in OPCs.

In the OL lineage, two GPCRs regulate the timing of CNS myelination. Gpr17, which is primarily expressed in OLs (79%) with some expression in OPCs (21%), acts as a negative regulator of myelination. The early onset OL differentiation and myelination observed in Gpr17 null mice, and the reduced myelin observed in mice overexpressing Gpr17 indicate that this GPCR inhibits OL differentiation. Mechanistically, Gpr17 induces the expression and nuclear translocation of OL differentiation inhibitor ID2[102]. In the context of white matter injury, the total knockout of Gpr17 in mice promotes remyelination after lysolecithin-induced focal demyelinating injury which correlates with phosphorylation of Erk1/2. Orthogonal approaches to disrupting Gpr17 function, including pharmacological inhibition of Gpr17 with Pranlukast, also promotes remyelination by inducing EPAC1 expression to facilitate OL differentiation[103]. Like Gpr17, Gpr37

inhibits OL differentiation, although its expression is limited to OLs. Deletion of Gpr37 results in precocious OL differentiation and myelination due to increased nuclear translocation of Erk1/2. Gpr37 inhibits OL differentiation by suppressing the cAMP EPAC-dependent activation of Raf-MAP-Erk1/2[104]. Where these GPCRs are activated, and whether they might localize to the primary cilium in OL lineage cells, is unknown.

Contribution to the field

After WMI, myelin sheaths can be regenerated by OPCs that migrate into lesions, proliferate within lesions, and differentiate into myelin forming OLs[105]. Failure of this remyelination program contributes to ongoing neurological dysfunction, axonal loss, and disease progression. Regulatory mechanisms relevant to human developmental myelin disorders and in myelin regeneration remain unclear. In chapter two, I present data demonstrating that primary cilia are critical for the OPC response to white matter injury. These data delineate a role for primary cilia as signaling compartments controlling OPC proliferation during development and within demyelinated lesions, providing cellular and molecular insights into how OPCs sense and respond to demyelination. This work adds to previous descriptive studies of OPC primary cilia by identifying a signaling pathway activated in OPC primary cilia and how this pathway affects OPC biology. Primary cilia are Hh signal transducers in many vertebrate cells, so we initially hypothesized that loss of OPC cilia would result in dysregulated Hh signals. We show that in OPCs, Hh pathway activation is unaffected when cilia are lost. Instead, we demonstrate that loss of the primary cilium in OPCs causes a significant downregulation in genes associated with CREB1 binding sites and attenuation of cAMP levels. Overall, these studies present a novel signaling organelle for exploration in OPCs, while also adding to our understanding of signaling mechanisms regulating OPC biology in development and disease.

In chapter three, I discuss several key questions to extend our understanding of OPC cilia. An outstanding question in the field of ciliary biology is the extent to which primary cilia can control

mammalian cell biology. The true scope of the functional importance of cilia remains elusive. Published reports have studied ciliary proteomes to identify all signaling components localized to this specific compartment[106-108]. These studies have been executed in cell lines that can be easily manipulated and instructed to construct cilia. It is unknown whether these proteomes represent those of ciliated cells in primary tissues. I present preliminary data gathered in collaboration with Maxence Nachury's lab and Ruth Huttenhain. These data represent initial attempts to identify proteins that survey OPC primary cilia under homeostasis using a proximity labeling technique called cilia-APEX[106]. Uncovering the spectrum of molecules present in OPC primary cilia will add to existing catalogues of ciliary proteomes and provide insights into potential tissue-specific differences in composition and function exhibited by primary cilia.

Chapter 2: Primary cilia control OPC proliferation in white matter injury via Hedgehog-independent CREB signaling.

Kimberly K. Hoi[1], Wenlong Xia[1], Ming Ming Wei[1], Maria Jose Ulloa Navas[2], Jose-Manuel Garcia Verdugo[2], Maxence V. Nachury[3], Jeremy F. Reiter[4,5], Stephen P.J. Fancy[1,6]

[1]Department of Neurology, Department of Pediatrics, Division of Neuroimmunology and Glial Biology, Newborn Brain Research Institute, University of California at San Francisco, San Francisco, CA 94158, USA.

[2]Laboratorio de Neurobiología Comparada, Instituto Cavanilles, Universidad de Valencia, CIBERNED, TERCEL, Paterna 46980, Spain.

[3]Department of Ophthalmology, University of California San Francisco, San Francisco, CA 94143, USA.

[4]Department of Biochemistry and Biophysics, Cardiovascular Research Institute, University of California, San Francisco, San Francisco, California 94158, USA.

[5]Chan Zuckerberg Biohub, San Francisco, CA 94158, USA.

[6]Correspondence: stephen.fancy@ucsf.edu

Summary

Remyelination after white matter injury (WMI) often fails in diseases such as multiple sclerosis due to improper recruitment and repopulation of oligodendrocyte precursor cells (OPCs) in lesions. How OPCs elicit specific intracellular programs in response to a chemically and mechanically diverse environment to properly regenerate myelin remains unclear. OPCs construct primary cilia, specialized signaling compartments that transduce Hh and GPCR signals. We investigated the role of primary cilia in the OPC response to WMI. Removing cilia from OPCs genetically via deletion of Ift88 resulted in OPCs failing to repopulate WMI lesions because of reduced proliferation. Interestingly, loss of cilia did not affect Hh signaling in OPCs or their responsiveness to Hh signals, but instead led to dysfunctional cAMP-dependent CREB-mediated transcription. As inhibition of CREB activity in OPCs reduced proliferation, we propose that a GPCR/cAMP/CREB signaling axis initiated at OPC cilia orchestrates OPC proliferation during development and in response to WMI.

Introduction

Damage to axons and myelinating oligodendrocytes (OL) in white matter injury is an important component of Multiple Sclerosis (MS) in adults as well as newborn brain injuries that cause cerebral palsy and cognitive disabilities. Damaged myelin sheaths can be regenerated in both conditions, but human myelin repair is highly susceptible to failure. Successful remyelination and functional recovery of axons depends on adequate oligodendrocyte precursor cell (OPC) recruitment into lesions[109, 110], involving their significant proliferation in response to injury. Indeed, OPC depletion and inadequate recruitment are hallmarks of many chronically demyelinated lesions[18, 19]. CNS developmental myelination also requires that OPCs proliferate, migrate, and decide either to differentiate or remain a precursor in the appropriate spatiotemporal manner[19, 21, 111]. Mechanisms regulating oligodendrocyte (OL) development have been studied extensively, resulting in the identification of both intrinsic and extrinsic factors that govern OPC migration,

19

proliferation, and differentiation[112]. However, as OPCs do not reside in a well-defined niche due to their distribution and tiling[113], it is unclear how OPCs are able to translate interactions with extracellular cues into specific intracellular responses in the context of the chemically and mechanically dense environments that exist in both development and remyelination.

Signaling specificity is often achieved via the spatial compartmentalization of signaling pathway components. The primary cilium is a specialized signaling organelle that manifests as a slender protrusion of the cell membrane that is found on most vertebrate cells. The ciliary membrane surrounds an axoneme with a 9+0 microtubule arrangement that is separated from the rest of the cell body via a transition zone, establishing a ciliary compartment[114]. Proteins are transported bidirectionally along the ciliary axoneme through the conserved process of intraflagellar transport (IFT). IFT thus plays a crucial role in assembly and maintenance of the ciliary axoneme[63-65]. In partnership with IFT, ciliary anterograde and retrograde transport are mediated by kinesin II and cytoplasmic dynein complex, respectively. Kinesin-II, comprised of KIF3A, KIF3B, and KAP3, is crucial in the construction and maintenance of the primary cilium, but also has critical extraciliary cytoskeletal roles.

Once thought of as vestigial organelles, primary cilia are now appreciated as specialized signaling organelles with critical roles in the transduction of mammalian Hh[67, 72] and GPCR signaling[59, 115]. When Hh ligand binds to Ptch1, Smoothened (Smo) accumulates in the cilium resulting in the activation of Gli transcriptional effectors. In the absence of Hh, Gli transcription factors are processed into their repressor forms (GliR) to keep Hh signals off[67]. In support of this, disruption of ciliogenesis often results in phenotypes associated with the gain or loss of Hh[74, 116]. Primary cilia have also been established as critical G-protein coupled receptor (GPCR) signaling centers[69], with an expanding subset of GPCRs and their effector molecules localizing to cilia, including SSTR3[77, 78] and GPR161[68, 107]. Ligand binding results in the activation of heterotrimeric G-proteins to either stimulate or inhibit cAMP production in the cell. Recently, it has been

discovered that vertebrate cells are able to distinguish between ciliary and extraciliary GPCR signaling and cAMP[66], providing further depth to the versatility and specificity of GPCR signaling. Primary cilia have been described in OPCs *in vitro*[92] and in the adult mouse *in vivo*[93, 94]. Deletion of Kif3a from OPCs in adult mice resulted in impaired proliferation in response to learning of a skilled motor task[93]. The function of cilia in white matter injury repair and signals transduced by OPC cilia remain poorly understood. Hh signaling is required for the specification of OPCs during embryonic development[32, 117]. Studies involving the overexpression of Shh in the adult CNS suggest that oligodendroglial lineage cells are responsive to Shh signals after focal demyelination[97, 98]. Others report stage specific Hh regulation of OLs during development, showing that continued expression of Smo in OPCs promotes proliferation while inhibiting differentiation[96]. Several GPCRs have also been implicated in regulating OL development. Gpr17 intrinsically regulates oligodendrocyte differentiation and timing of myelination[102], while Gpr56[100, 101] regulates OPC proliferation.

We investigated the function of ciliary signaling in OPC development and white matter injury repair. Here we show that OPC cilia are required for and control proliferation during development and in response to focal demyelinating injury, by regulating CREB-mediated transcription but not Hh signaling.

Results

OPCs are ciliated in mammalian CNS development and white matter injury

Previous studies indicate that OPCs are ciliated *in vitro* and in the adult mouse brain *in vivo*[92, 93]. We sought to determine whether OPC cilia may be relevant to human white matter injury repair and found that human OPCs in this context are ciliated, shown as Arl13b-labeled primary cilia in OLIG2$^+$ cells from human neonatal hypoxic ischemic encephalopathy (HIE) (**Figure 2.1a**). To confirm the presence of cilia in OPCs morphologically, we performed electron microscopy in NG2-EGFP mice at P60, where OPCs (which express NG2) are labeled with EGFP, allowing for

identification of OPCs in electron micrographs via immunogold labeling. OPC cilia can be clearly seen on EM, displaying the basal body, axoneme, and ciliary pockets (**Figure 2.1b**). We also confirm the presence of cilia on OPCs, but not mature OLs, in OPCs purified from P7 WT mice (**Figure 2.1c**).

To determine whether OPC ciliation changes throughout CNS development, we quantified the proportion of OPCs with cilia at different developmental time points. At E13.5 in the developing mouse brain, 67.22% $\pm$ 3.67 OPCs are ciliated. This is reduced to 49.69 $\pm$ 4.71% at P0 and 35.21% $\pm$ 1.97% at P7 before stabilizing at 49.56 $\pm$ 0.75% and 48.56% $\pm$ 6.14% at P21 and P60, respectively. The reduction of ciliated OPCs is likely due to proliferation and the previously characterized deconstruction of primary cilia as cells, including OPCs, enter the cell cycle[61]. A similar trend was observed in the developing mouse spinal cord. At E13.5, 83.85 $\pm$ 8.61% of OPCs harbored cilia, which decreased to 35 $\pm$ 7.64% at P7, and increased to 41.03 $\pm$ 3.14% at P60 (**Figure 2.1d-e**). Similar to our results in purified OPCs, mature OLs in the P7 mouse cortex do not harbor primary cilia (**Figure 2.1d**), suggesting that cilia are deconstructed before or during differentiation.

We characterized OPC ciliation in white matter injury using an established lysolecithin-induced mouse model of demyelinating injury. We assessed lesions in the dorsal funiculus of the adult mouse spinal cord at 5-days post-lesion (5dpl) and found that OPCs are also ciliated in mouse white matter injuries. In the white matter that surrounds the lesion core, 43.30 $\pm$ 1.68% of OPCs are ciliated, a similar proportion to what we observed in the uninjured P60 spinal cord. Within the demyelinated lesions, 19.08 $\pm$ 1.86% of OPCs harbor cilia (**Figure 2.1f**). The reduced percentage of ciliated OPCs within the lesion at 5dpl reflects the well-characterized rapid proliferation of OPCs at this timepoint in this injury model. Ciliogenesis is tightly coupled to the cell cycle. Deconstruction of the ciliary axoneme occurs during cell division to allow the centrosome (the basal body) to fulfill its role as a microtubule organizing center. Cilia are then

reconstructed after cell division[61]. The presence of ciliated OPCs within lesions indicates that OPCs can be responsive to signals transduced through cilia after white matter injury.

Removing cilia from OPCs prevents proliferation during development

To assess whether primary cilia function in oligodendroglial development, we removed cilia in OPCs by genetically deleting a critical component of ciliary maintenance. Deletion of components involved in IFT, such as Ift88, results in disrupted ciliogenesis, effective loss of primary cilia, and loss of ciliary signaling. We generated PDGFRα-Cre: Ift88$^{fl/fl}$; RosaEYFP mice (referred to as Ift88 cKO hereafter), in which OPCs with Ift88 conditionally deleted express EYFP (labeled with GFP). Littermates expressing PDGFRα-Cre and possessing a WT Ift88 allele (PDGFRα-Cre: Ift88$^{fl/wt}$; RosaEYFP) served as controls. We used EYFP to verify that recombination in these mice occurs in OPCs expressing Pdgfrα (**Figure 2.2a**). Conditional removal of Ift88 from EYFP$^+$ OPCs resulted in a 90% reduction in ciliated EYFP$^+$ OPCs (EYFP$^+$Arl13b$^+$) (**Figure 2.2b**).

By P7, OPCs are well distributed across the mouse brain in wildtype mice and have begun to differentiate in the white matter but are still highly proliferative in the cortex. Ift88 cKO mice, however, exhibited a 40% reduction in the density of EYFP$^+$ OPCs in the P7 cortex compared to controls (**Figure 2.2c**). Despite this, the number of total Pdgfrα$^+$ OPCs in the P7 Ift88 cKO cortex remained unchanged compared to controls. This was due to a compensatory increase in the proliferation of EYFP negative OPCs that still harbored cilia (**Figure 2.3a**), which reflects the propensity for OPCs to tile and divide to replace missing neighboring OPCs[113]. As non-recombined, ciliated EYFP$^-$ OPCs compensate for diminished EYFP$^+$ OPCs, our study focuses on the EYFP$^+$ cells in Ift88 cKO and controls.

To determine whether the reduction in the density of EYFP$^+$ Ift88 cKO OPCs was due to defects in OPC proliferation upon loss of cilia, we administered the thymidine analog 5-ethynyl-2'-deoxyurdine (EdU) at P7 and P8 to label dividing cells and analyzed cortices at P11 (**Figure

2.2d). We detected a significant reduction in the fraction of EdU$^+$EYFP$^+$ OPCs (50%) (**Figure 2.2e**) in Ift88 cKO, indicating that the population of OPCs lacking cilia fail to expand. OPCs in Ift88 cKO displayed no significant difference in expression of cell death markers cleaved caspase 3 or TUNEL (**Figure 2.4a-b**), which shows that the loss of OPC cilia does not affect OPC survival. Furthermore, we found that loss of OPC cilia did not affect the ability of OPCs to differentiate (**Figure 2.3c**). Taken together, these results demonstrate that loss of OPC cilia prevents OPC proliferation during CNS development.

Primary cilia are required for OPC proliferation in remyelination.

Remyelination following white matter injury (WMI) is highly susceptible to failure in diseases such as MS and newborn hypoxic brain injury, but regulatory factors relevant in human myelin regeneration are unclear. Successful remyelination requires the recruitment of OPCs into areas of demyelination and their significant intralesional proliferation. To assess the function of primary cilia in OPC proliferation following WMI, we used tamoxifen inducible PDGFRα-CreERT: ift88$^{fl/fl}$; RosaEYFP mice (referred to as Ift88 icKO hereafter) to remove cilia from adult mice while avoiding developmental defects that may arise from constitutive loss of OPC cilia. Littermates expressing PDGFRα-CreERT and one WT Ift88 allele were used as controls. We induced recombination in these mice by administrating tamoxifen at 4 weeks of age and verified that our tamoxifen injection paradigm resulted in recombination in OPCs in the adult mouse spinal cord using EYFP (**Figure 2.5a-b**). We then produced a focal demyelinated lesion in the mouse spinal cord in 10-week-old Ift88 icKO and controls and assessed the lesion at 5 days post lesioning (5 dpl) when peak OPC recruitment occurs in this WMI model. We confirmed that the removal of Ift88 resulted in a 75% reduction in the proportion of ciliated EYFP$^+$ OPCs (EYFP$^+$Arl13b$^+$) in lesions (**Figure 2.5c**). Loss of OPC cilia also resulted in a significant 50% reduction in the density of EYFP$^+$ OPCs populating the lesion (**Figure 2.5d**) in Ift88 cKO compared to controls. However, as in development, the total number of Pdgfrα$^+$ cells within Ift88 icKO lesions remained the same

as in controls, which we attribute to incomplete recombination in adult OPCs and a compensatory increase in the proliferation of EYFP⁻OPCs that still have cilia (**Figure 2.3b**). Our analyses therefore focused on the EYFP⁺ population of cells in lesions.

To determine whether OPC cilia are required for the local proliferation of OPCs in WMI, we performed lysolecithin lesions and then injected EdU IP at 3dpl for subsequent assessment at 5dpl in Ift88 icKO and controls. Removal of OPC cilia reduced the number of proliferating OPCs in lesions by 50% (EYFP⁺EdU⁺: $31.38 + 1.69\%$ in controls vs. $15.50 + 3.14\%$ in Ift88 cKO) (**Figure 2.5e**). We observed no significant difference in OPCs expressing cleaved caspase 3 or TUNEL, indicating that loss of OPC cilia did not affect OPC survival signaling during lesion repair (**Figure 2.4c-d**). These results indicate that primary cilia are required for the OPC response to injury and function to promote OPC expansion within WM lesions.

Hedgehog activity is unaffected by the loss of OPC cilia.

Vertebrate primary cilia activate GLI transcription factors and generate GLI transcriptional repressors to regulate Hh signaling[67, 74, 115, 118]. While there is strong evidence for the role of Hh signaling in OPC specification, there remain conflicting reports of the role of this signaling pathway in oligodendroglial proliferation, differentiation, and involvement in injury repair. To assess whether primary cilia control Hh signaling in OPCs, we examined the expression of two Hh target genes, *Gli1* and *Ptch1*. Quantitative RT-PCR analysis of OPCs isolated via immunopanning from P7 Ift88 cKO and control mice revealed no significant difference in *Gli1* or *Ptch1* expression in OPCs lacking cilia (**Figure 2.6a**). Due to the sustained expression of Hh target genes in Ift88 cKO, we sought to determine whether OPCs that have lost cilia are responsive to Hh signals. We treated OPCs isolated from P7 control and Ift88 cKO mice with 0, 10, or 50 nM Smoothened Agonist (SAG) in cell media. This was followed by treatment with EdU to label proliferating cells. Consistent with the observations from our *in vivo* studies, isolated Ift88 cKO OPCs exhibited a decrease in proliferation compared to controls in 0 nM SAG (**Figure 2.6b**). Interestingly, treatment

with 10 or 50 nM SAG resulted in the increased proliferation of both control and Ift88 cKO OPCs (**Figure 2.6b**). We assessed *Gli1* and *Ptch1* expression in OPCs after SAG treatment via qRT-PCR and established that *Gli1* and *Ptch1* expression increased in both control and Ift88 cKO OPCs in the presence of 10 and 50 nM SAG (**Figure 2.6c-d**). Together, these results show that Hh signaling is unaltered in Ift88 cKO OPCs, possibly due to extraciliary Smoothened activation. Furthermore, these data point toward a non-Hh mechanism of signal transduction in OPC cilia responsible for regulating proliferation.

The primary cilium controls OPC proliferation via regulation of CREB activity.

To establish the signaling pathways affected in OPCs after removal of cilia, we used RNA sequencing (RNA-seq) to transcriptionally profile OPCs isolated from the cortices of P11 Ift88 cKO mice and controls by FACS (via endogenous EYFP expression). We identified 443 significantly upregulated and 566 significantly downregulated (p<0.05) genes in Ift88 cKO OPCs compared to control OPCs. Our RNA-seq data confirmed that loss of OPC cilia did not alter the expression of common Hh targets *Gli1, Gli2, Gli3,* and *Smo* (**Figure 2.7b**). We compared our generated list of downregulated genes with existing ChIP-X datasets using Enrichr (https://maayanlab.cloud/Enrichr/enrich#). We noticed a significant overlap in genes associated with the cyclic AMP (cAMP) response element-binding protein 1 (CREB1) binding site (adjusted p-value 6.8E-06) between our downregulated genes and transcription factors present in ENCODE and ChEA (**Figure 2.7a**). Analysis of the significantly downregulated CREB1-associated genes from our dataset through literature search revealed that *Hlf*, *Pde4a*, *Rnf40, Herc2*, *Eif3a, Jarid2*, *Cdkn1a*, *Becn1*, and *Id1* have been previously linked to cell cycle control and proliferation (**Figure 2.7b**)[118-125]. qRT-PCR analysis of purified P7 Ift88 cKO and control OPCs confirm that loss of OPC cilia decreases the expression of these genes (**Figure 2.7c**).

We explored the possibility that loss of OPC cilia affects CREB activity in OPCs. The initiation of CREB-dependent transcription requires CREB activation through phosphorylation by

protein kinases[126]. OPCs isolated from P7 Ift88 cKO exhibited reduced expression of phosphorylated CREB (pCREB) (Ser133) compared to controls, suggesting that removal of OPC cilia inhibits CREB activation (**Figure 2.7d**). To determine whether OPC proliferation requires CREB activation and subsequent CREB-mediated gene transcription, we used 666-15, a cell-permeable naphthol derivative and selective inhibitor of CREB-mediated gene transcription[127]. OPCs isolated from P7 WT rats displayed a significant reduction in proliferation when treated with 50 nM 666-15 compared to control DMSO (**Figure 2.7e**). 666-15 reduced pCREB (Ser133) expression in OPCs (**Figure 2.7g-h**) and gene expression of several of the differentially expressed CREB-associated genes identified from our RNA-seq analysis: *Rnf40, Herc2, Eif3a, Jarid2* (**Figure 2.7i**), as analyzed via qRT-PCR. If CREB-mediated gene transcription regulates OPC proliferation, we hypothesized that selected CREB1-associated genes from our transcriptional analysis of Ift88 cKO OPCs would also be required for OPC proliferation. We generated shRNAs to silence the expression of these genes in P7 WT rat OPCs *in vitro*. Of these, knockdown of *Eif3a* and *Jarid2* significantly reduced OPC proliferation (**Figure 2.8**). Silencing *Cdkn1a* expectedly increased OPC proliferation (**Figure 2.8**), as *Cdkn1a* suppresses proliferation by inhibiting cell cycle progression[124].

CREB1 is a downstream effector of cAMP, a secondary messenger involved in signaling cascades triggered by GPCRs. As a growing number of GPCRs are identified to be specifically targeted to mammalian cilia, the downregulation of genes associated with CREB1 binding in Ift88 cKO may indicate that loss of OPC cilia results in defective GPCR and cAMP signaling in OPCs. To determine whether the reduction of CREB activation observed in OPCs upon loss of cilia is due to attenuated cAMP production, we assessed cAMP levels in OPCs *in vitro* using a cAMP-Glo Assay. Purified Ift88 cKO OPCs displayed a reduction in intracellular cAMP levels (**Figure 2.7j**). Overall, our data show that in the absence of cilia, OPCs fail to proliferate due to attenuated cAMP levels and, consequently, decreased CREB-mediated transcription of genes linked to proliferation (e.g., *Jarid2* and *Eif3a*). Since cAMP notably lies downstream of GPCRs, this study

points to a GPCR/cAMP/CREB signaling axis that is initiated at OPC primary cilia to promote OPC proliferation.

Discussion

After insult to white matter, remyelination involves the enhanced migration, proliferation, and differentiation of OPCs in areas of injured and recovering tissue. The regeneration of myelin therefore depends upon OPC activation and proliferation, but OPCs often remain depleted in chronically demyelinated lesions[18, 19]. While the environmental and intrinsic systems regulating OPC proliferation have been studied extensively in development, these studies are sparser in the context of injury. Processes regulating developmental myelination are often recapitulated during remyelination, and factors controlling OPC proliferation during development can promote myelin regeneration after injury[110]. For instance, PDGF, FGF, and EGF are all factors that have been shown to promote proliferation during development and in response to different models of WMI through their obligate receptors (PDGFRα, FGFRs, and EGFRs)[40, 42, 128, 129]. In this study, we find that remyelination requires OPC cilia and ciliary signaling, as loss of cilia significantly reduces OPC proliferation in white matter lesions.

Primary cilia most commonly transduce Hh signals. In cultured rat OPCs, ciliobrevin, an AAA+ ATPase inhibitor that also causes cilia disassembly, destabilized OPCs while co-treatment with ciliobrevin and Shh preserved OPC morphology and ciliary assembly[92]. However, whether OPC cilia are required for Hh signal transduction has not previously been studied. In addition to the critical role of Hh in embryonic OPC specification[32, 130], several studies show that overexpression of Shh in the adult mouse corpus callosum under homeostatic conditions and after focal demyelination promoted Hh gene expression, OPC proliferation, and tissue preservation[97, 98], indicating that OPCs are responsive to Hh signals under different contexts. Surprisingly, our results show that cilia are not required for Hh signal transduction in OPCs. How are OPCs transducing Hh signals without the requisite ciliary accumulation of Smo? One possible

explanation is that Hh pathway activation can occur in the absence of ciliary Smo accumulation. In the absence of OPC cilia, Hh ligand could be engaging extraciliary Smo activity to regulate Gli and promote Hh target gene expression[131]. Loss of cilia in OPCs produces proliferation deficits with intact Hh signaling, pointing toward Hh-independent ciliary control of OPC proliferation.

This study reveals that loss of OPC cilia results in the downregulation of genes associated with CREB binding sites. CREB phosphorylation can occur in response to mitogens and the function of CREB activation has been linked to proliferation in many cell types[132, 133]. In oligodendrocyte lineage, OPC proliferation follows the rapid stimulation of CREB phosphorylation upon exposure to neurotrophin (NT-3)[134]. Our data are consistent with previous studies showing that CREB-mediated transcriptional changes can promote the proliferation and population maintenance of OPCs[135]. Still, CREB can be activated by a wide variety of stimuli yet evoke extremely specific responses depending on the selective initiation of downstream gene transcription. The CREB response to signaling initiated at the cilium likely involves the transcription of a specific subset of factors that regulate proliferation and differ from gene transcription initiated from extraciliary signals. We identify *Eif3a* and *Jarid2* as genes downstream of ciliary CREB activation in OPCs, but their roles in oligodendrocyte biology are not defined. Studies in several cell types show that knockdown or mutations in *Eif3a* or *Jarid2* result in decreased proliferation[122, 123], providing a precedent for their role in promoting OPC proliferation.

To fully define the ciliary contribution to OPC proliferation would require the identification of ciliary-localized upstream regulators of CREB activation. CREB lies downstream of kinases that are activated as a part of the cAMP signaling cascade. As cAMP is the secondary effector for GPCR signal transduction, and GPCRs are enriched in primary cilia, a ciliary GPCR may be mediating OPC proliferation. Indeed, several GPCRs control OL development. GPR37, enriched in promyelinating and mature OLs but not OPCs, inhibits precocious myelination by inhibiting the cAMP/EPAC activation of ERK1/2[104]. Gpr17 also inhibits myelination, but via the upregulation of myelination inhibitors ID2/4[102]. GPR56, an adhesion-GPCR, maintains OPC proliferation and

inhibits differentiation in a RhoA-dependent manner[100, 101]. As Gpr17 and Gpr56 are expressed in OPCs, it would be interesting to determine whether they are enriched in OPC primary cilia. Multiple functional GPCRs could localize to OPC cilia. Instead of a straightforward model where one ciliary GPCR acts independently to affect changes in OPC biology, the intracellular changes observed upon removal of cilia in OPCs could be due to loss of a well-choreographed crosstalk between multiple ciliary GPCRs that fine tune cAMP levels either in the cytoplasm or ciliary axoneme through enlisting a balance of stimulatory and inhibitory G-protein subunits. This adds yet another way in which signaling specificity can be achieved by OPCs.

While our study identifies a novel mechanism whereby signal transduction via OPC cilia activates CREB-mediated transcription to promote OPC proliferation, the true scope of the functional importance of OPC cilia remains unclear. The ciliary membrane is physically contiguous with the plasma membrane but molecularly distinct due to a transition zone at the base of the cilium that regulates protein trafficking in and out of the organelle[136]. With advancements in proximity labeling technologies, it is now possible to consistently isolate and analyze proteins selectively localized to primary cilia[106, 107]. Studies show that the composition of cilia can be dynamic[107, 137] and clearly differs between cell types. For example, adenylate cyclase 3 is present in neuronal cilia but is not detected in IMCD3 kidney cells[106]. The ciliary transition zone has also been shown to display compositional differences between cell types[138]. Furthermore, ciliary GPCRs display regional specificity, as exemplified by differences in neuronal ciliary expression of somatostatin receptor 3[77], the serotonin receptor 5-HT$_6$[84], and melanocortin 4 receptor[79]. The compositional diversity of cilia across cell types highlights the potential for unique, cell type-specific ciliary proteomes. Identification of signaling proteins specific to OPC cilia, and the downstream signaling cascades, may provide fascinating insights into how specialized signaling occurs in OPCs. It will also contribute to the identification of drug targets to promote OPC proliferation in white matter diseases.
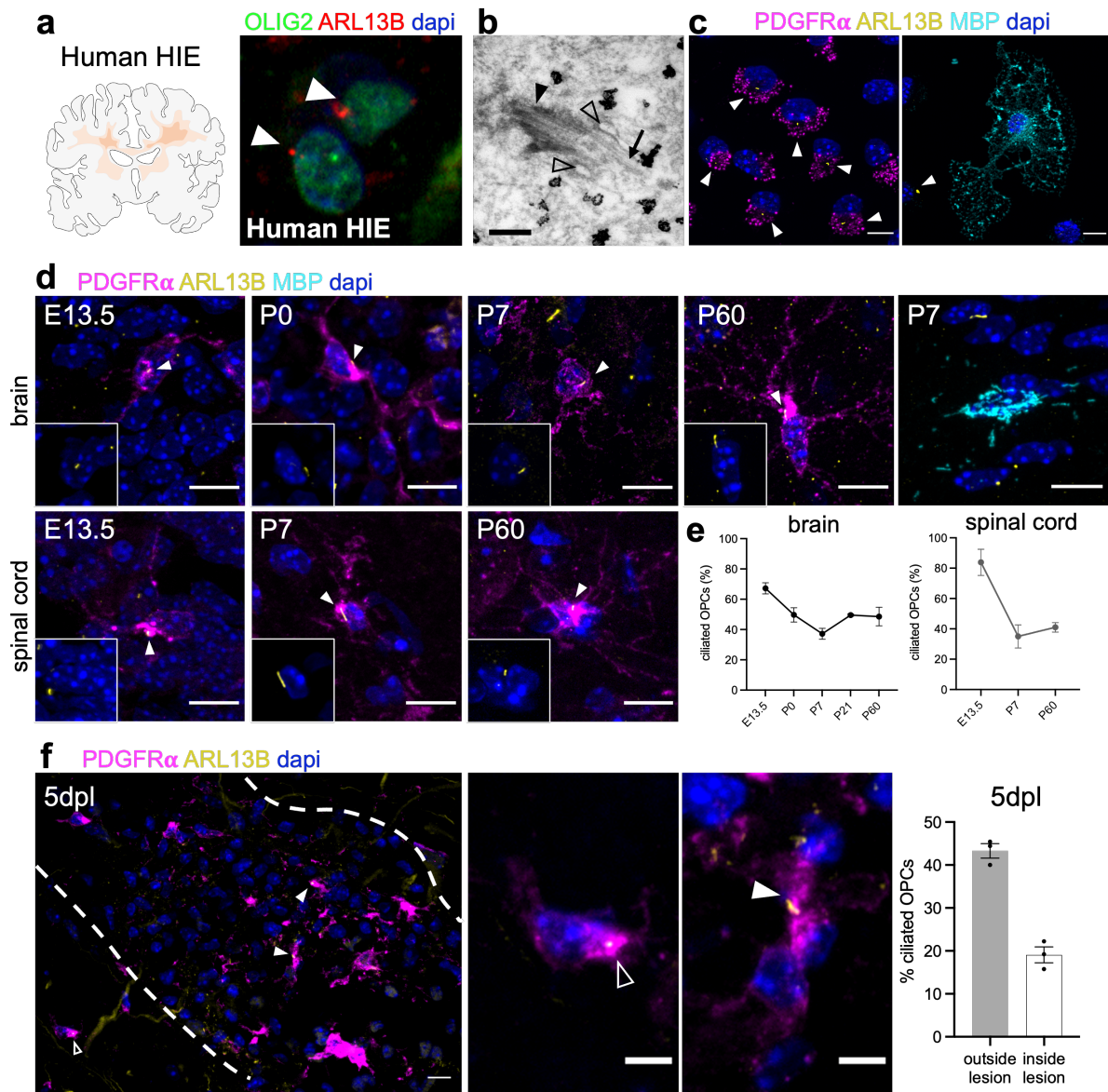
Figure 2.1. OPCs are dynamically ciliated during development and injury.

(a) Immunofluoresence for cilia (Arl13b, red) in oligodendrocyte lineage cells (Olig2, green) in tissue collected from human HIE.

(b) Electron micrograph of cilia in OPCs labeled with immunogold GFP from P60 NG2-EGFP mice. Scale bar, 200 nm. Black arrow: axoneme, black arrowhead: basal body, empty arrowhead: ciliary pockets.

(c) Immunofluorescence for cilia (Arl13b, yellow) in OPCs (Pdgfrα, magenta) and mature OLs (MBP, cyan) isolated from P7 rats. Arrowheads mark ciliated OPCs. Nuclei are labeled with DAPI. Scale bars, 10 μm.

(d) Immunofluorescence for cilia (Arl13b, yellow) in OPCs (Pdgfrα, magenta) and mature OLs (MBP, cyan) at the indicated time points in the developing mouse brain (top row) and spinal cord (bottom row). Arrowheads mark ciliated OPCs. Nuclei are labeled with DAPI. Scale bars, 10 μm.

(e) Quantifications of the percentage of ciliated OPCs over total OPCs across different time points in mouse brain and spinal cord development. n=4-5 mice per time point.

(f) Immunofluorescence and quantifications for cilia (Arl13b, yellow) and OPCs (Pdgfrα, magenta) at 5 days post-lysolecithin lesion in the adult mouse spinal cord dorsal funiculus. Arrowheads mark ciliated OPCs. Nuclei are labeled with DAPI. Scale bars, 50 µm and 5 µm (inset).
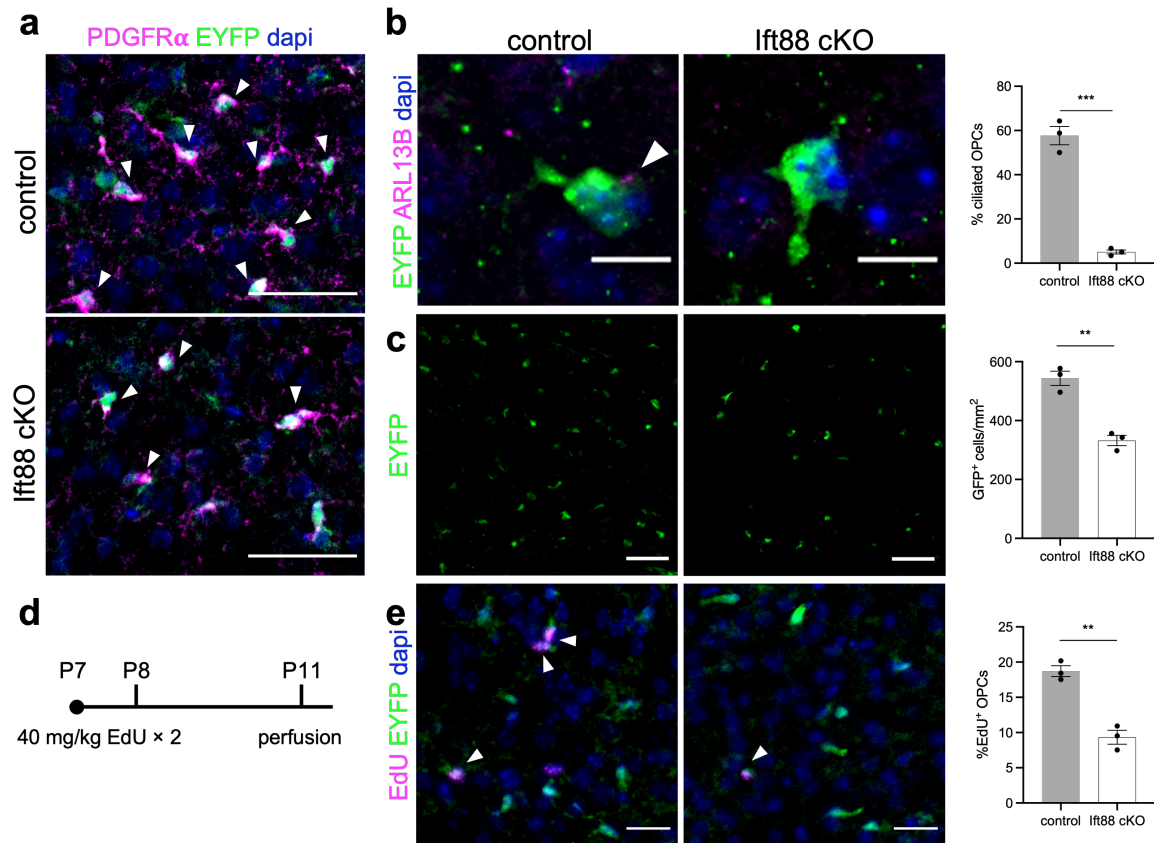
Figure 2.2. Disruption of ciliogenesis reduces OPC expansion in the developing mouse cortex. (a) Detection of EYFP (green) in OPCs (arrowheads; Pdgfrα, magenta) in P7 Pdgfrα-Cre: Ift88[fl/wt]; RosaEYFP (control) and Pdgfrα-Cre: Ift88^{fl/fl}; RosaEYFP (Ift88 cKO) mice. Scale bar, 50 μm.
(b) Detection and quantification of cilia (Arl13b, magenta) in OPCs (EYFP, green) from control and Ift88 cKO mice. n=3 mice per genotype. Data are represented as mean $\pm$ SEM.
(c) Representative images of recombined OPCs (EYFP, green) in the cortex of control and Ift88 cKO mice at P7. Scale bar, 50 μm. Quantification of EYFP$^+$ OPC density (calculated per mm^2) in the cortex of control and Ift88 cKO mice at P7. n=3 mice per genotype. P=0.0021. Difference between means -211.2 ± 29.97. 95% confidence interval -294.4 to -127.9.
(d) Experimental paradigm for EdU injections in the developing mouse cortex.
(e) Representative images of EdU (magenta) and OPCs (EYFP, green) in the cortex of control and Ift88 cKO animals, with arrows indicating colocalized EdU$^+$EYFP$^+$ cells. Scale bar, 25 μm. Quantification of GFP$^+$ OPCs that are EdU$^+$, calculated by percentage of EdU$^+$EYFP$^+$ (EdU, magenta; EYFP, green) cells over total EYFP$^+$ cells at P11. n=3 mice per genotype. For (b), (c), and (e), significance was determined via unpaired t-tests. A p-value less than 0.05 was considered statistically significant, with significance denoted with the following symbols: **p<0.01 and ***p<0.001. Data are represented as mean $\pm$ SEM.
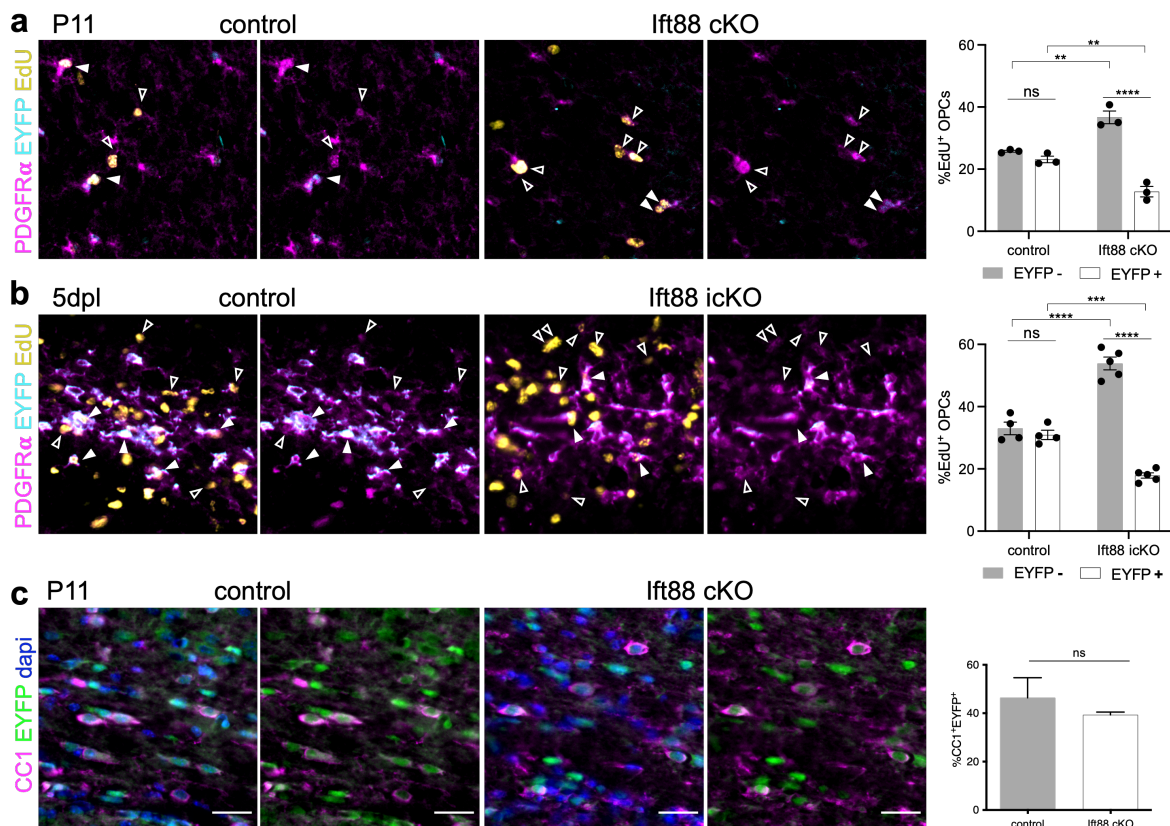
Figure 2.3. Proliferation of EYFP-negative OPCs compensates for reduced proliferation of EYFP+ OPCs during development and 5dpl.

(a) Representative images of immunofluorescence for OPCs (Pdgfrα, magenta), EYFP (cyan), and EdU (yellow) in control and Ift88 cKO mice at P11. Quantifications show the percentage of proliferating EYFP-negative OPCs and proliferating EYFP+ OPCs. n=3 mice per genotype.

(b) Representative images of immunofluorescence for OPCs (Pdgfrα, magenta), EYFP (cyan), and EdU (yellow) in lesions of control and Ift88 icKO mice 5dpl. Quantifications show the percentage of proliferating EYFP-negative OPCs and proliferating EYFP+ OPCs. n=4-5 mice per genotype. For (a) and (b), significance was determined via two-way ANOVA with Tukey's post-hoc analysis. A p-value less than 0.05 was considered statistically significant, with significance denoted with the following symbols: ns indicates not significant, **$p<0.01$, ***$p<0.001$, and ****$p<0.0001$. Data are represented as mean $\pm$ SEM.

(c) Representative images of differentiating OPCs (CC1, magenta and EYFP, green) in control and Ift88 cKO mice at P11. Quantifications show percentage of CC1+ EYFP+ OPCs. n=3 mice per genotype. Significance was determined via unpaired t-test. ns indicates not significant.
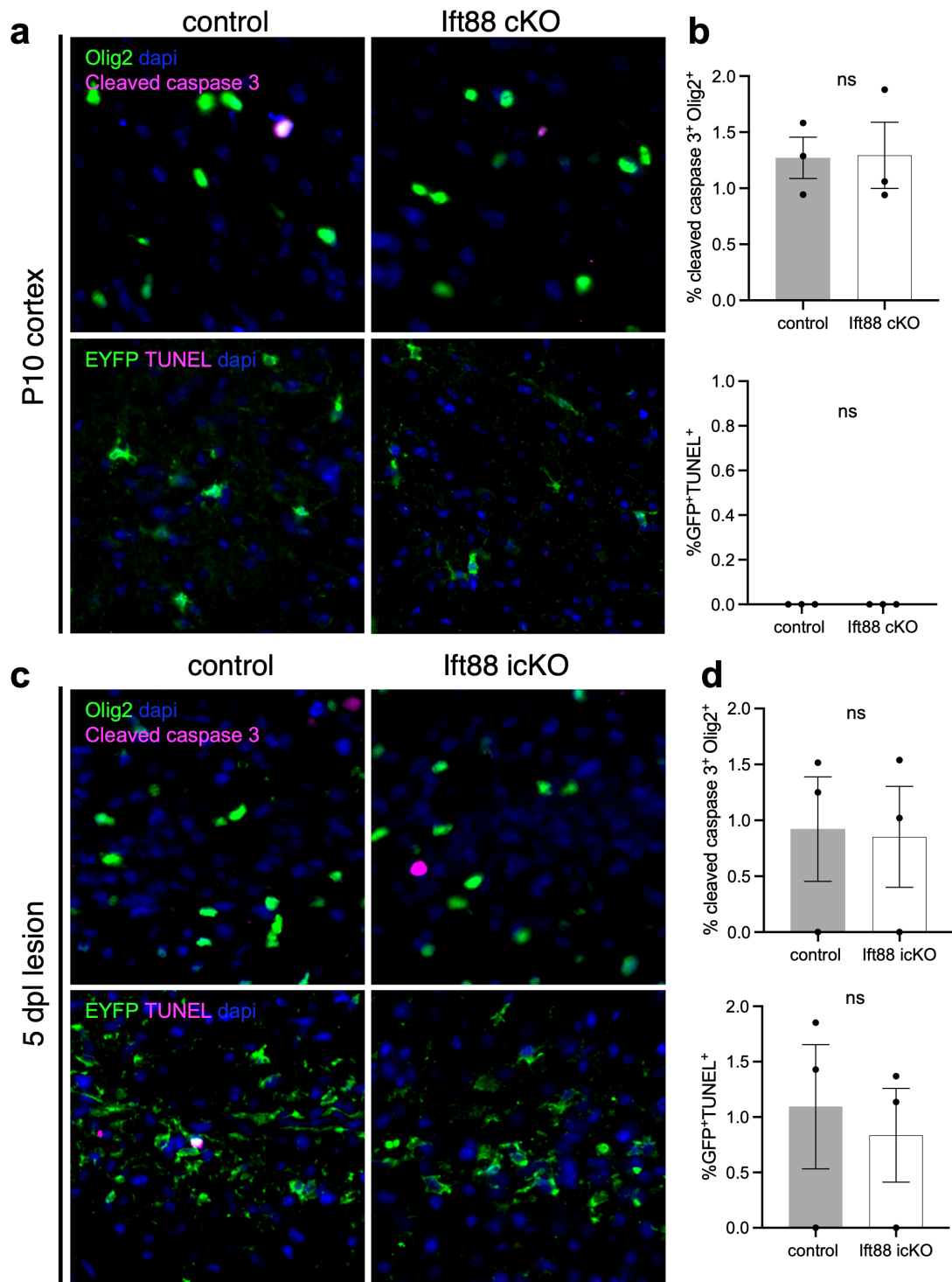
Figure 2.4. Loss of Ift88 does not result in increased OPC death in development or 5 dpl. (a) Cell death markers (cleaved caspase 3 or TUNEL, magenta) in oligodendrocyte lineage cells (Olig2 or EYFP, green) in the P10 Ift88 cKO cortex compared to controls. n=3 mice per genotype. (b) Quantification of (a). Cell death was quantified by percentage of cleaved caspase 3$^+$Olig2$^+$ over total Olig2$^+$ or TUNEL$^+$EYFP$^+$ over total EYFP$^+$. n=3 mice per genotype.

(c) Cell death markers (cleaved caspase 3 or TUNEL, magenta) in oligodendrocyte lineage cells (Olig2 or EYFP, green) in lesions at 5dpl in Ift88 icKO compared to controls.

(d) Quantification of (c). Cell death was quantified by percentage of cleaved caspase 3^+Olig2$^+$ over total Olig2$^+$ or TUNEL$^+$EYFP$^+$ over total EYFP$^+$. n=3 mice per genotype. For (b) and (d), significance was determined via unpaired t-tests. A p-value less than 0.05 was considered statistically significant, with significance denoted with the following symbols: ns indicates not statistically significant.
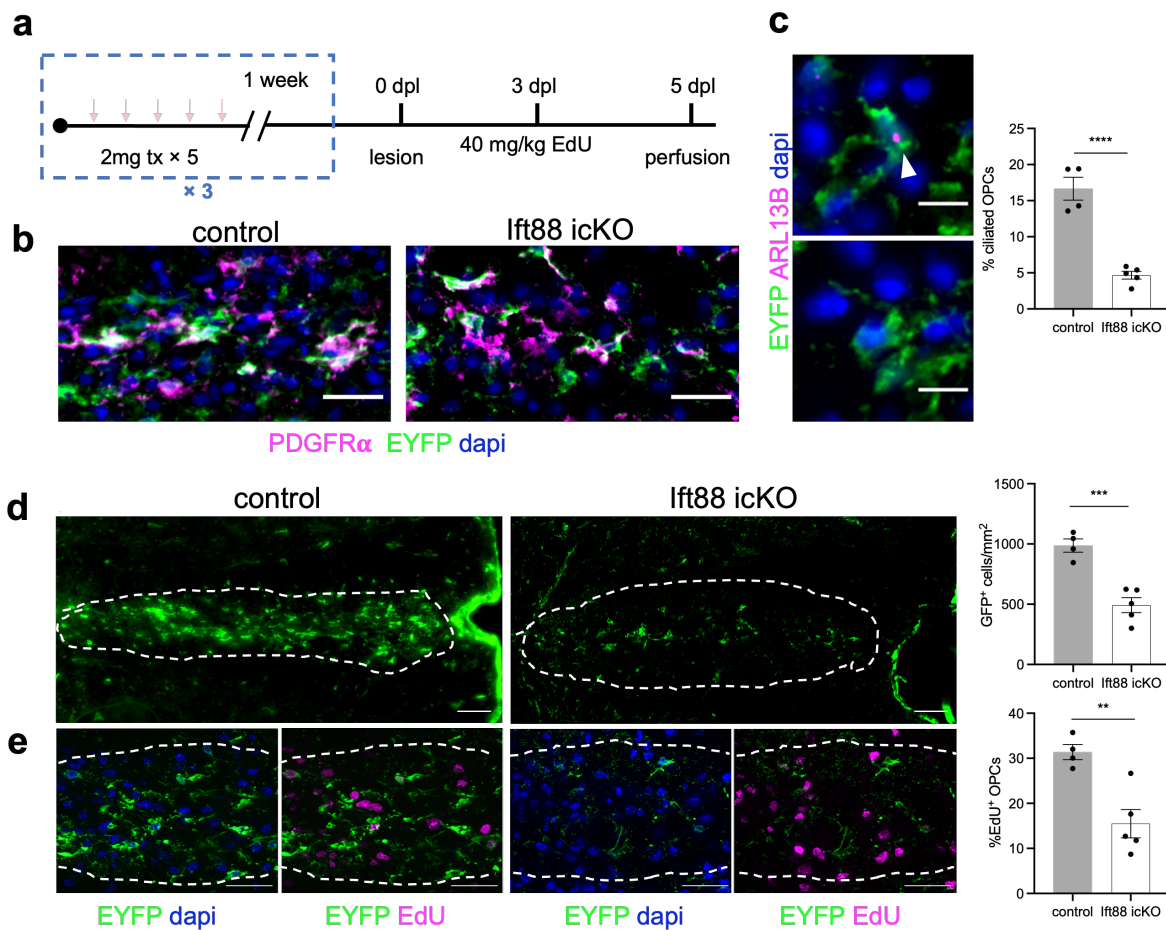
Figure 2.5. Disruption of ciliogenesis reduces OPC proliferation in white matter injury.

(a) Experimental paradigm for tamoxifen injections and lysolecithin lesions in Pdgfrα-CreERT: Ift88$^{fl/fl}$; RosaEYFP (Ift88 icKO) and control mice.

(b) Detection of EYFP (green) in OPCs (arrowheads; Pdgfrα, magenta) in dorsal funiculus lysolecithin lesions at 5dpl in control and Ift88 icKO mice.

(c) Detection and quantification of cilia (Arl13b, magenta) in OPCs (EYFP, green) within lesions from control and Ift88 icKO mice at 5 dpl.

(d) Representative images of recombined OPCs (EYFP, green) in dorsal funiculus lesions 5 dpl from control and Ift88 icKO mice. Scale bars, 50 μm. Quantification of EYFP$^+$ OPC density (calculated per mm^2) in 5dpl dorsal funiculus. n=4-5 mice per genotype. P=0.0007. Difference between means -495.1 ± 85.26. 95% confidence interval -696.7 to -293.5.

(e) Representative images of EYFP$^+$EdU$^+$ proliferating OPCs within lesions at 5dpl from control and Ift88 icKO mice. Quantification of EYFP$^+$ OPCs that are EdU$^+$, calculated by percentage of EdU$^+$EYFP$^+$ (EdU, magenta; EYFP, green) cells over total EYFP$^+$ cells in 5 dpl dorsal funiculus. n=4-5 mice per genotype. For (c), (d), and (e), significance was determined via unpaired t-tests. A p-value less than 0.05 was considered statistically significant, with significance denoted with the following symbols: **p<0.01, ***p<0.001, and ****p<0.0001. Data are represented as mean ± SEM.
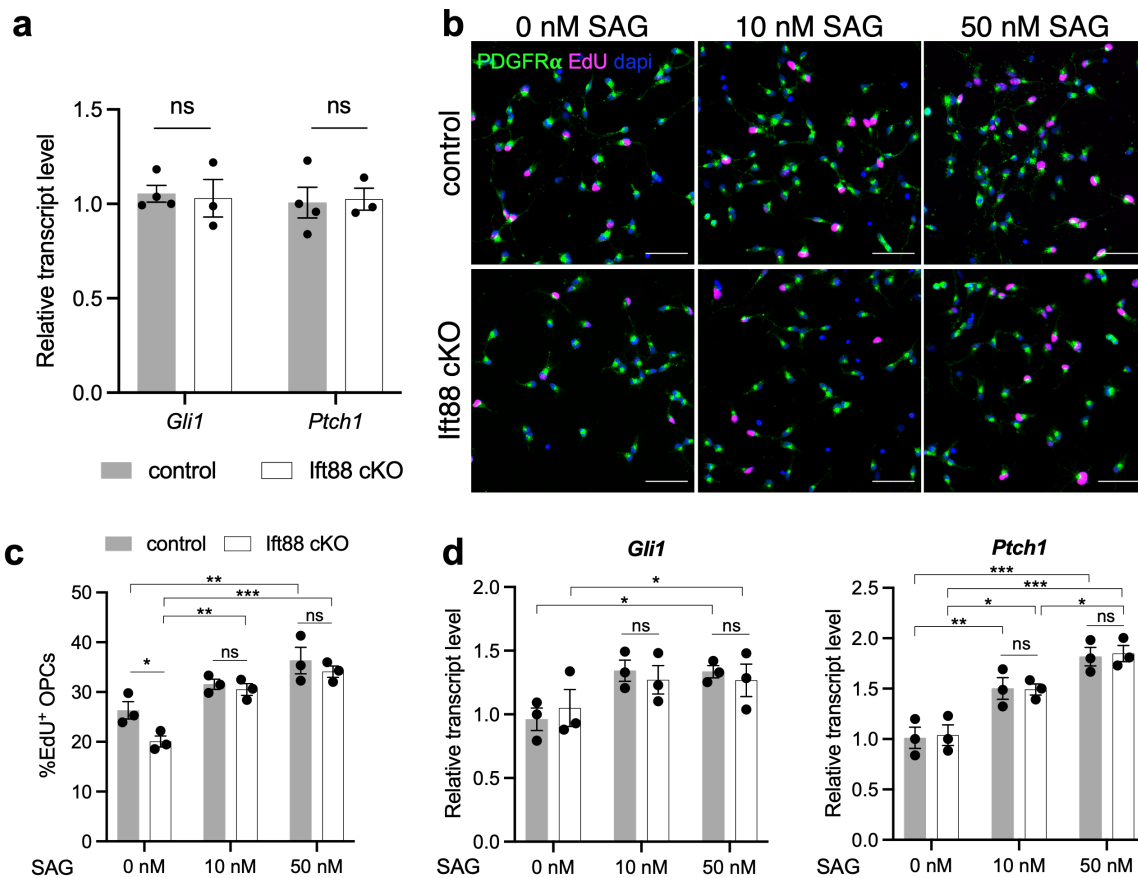
Figure 2.6. Hh activity is unaffected by the loss of OPC cilia *in vitro*.

(a) qRT-PCR of Gli1 and Ptch1 transcripts show no difference in expression between OPCs isolated from P7 control and Ift88 cKO mice. n= 3 mice per genotype.

(b) 10 nM and 50 nM of SAG promotes proliferation in both control and Ift88 cKO OPCs in vitro. Scale bars, 50 μm.

(c) Quantification of EdU⁺Pdgfrα⁺ (EdU, magenta; Pdgfrα, green) proliferating OPCs, calculated by percentage of EdU⁺Pdgfrα⁺ cells over total Pdgfrα⁺ cells. n=3 per genotype per condition.

(d) qRT-PCR of Gli1 and Ptch1 transcripts in OPCs after treatment with 10 nM and 50 nM SAG. n=3 per genotype per condition. For (c) and (d), significance was determined via two-way ANOVA with Tukey's post-hoc analysis. A p-value less than 0.05 was considered statistically significant, with significance denoted with the following symbols: ns indicates not significant, *$p<0.05$, **$p<0.01$, ***$p<0.001$, and ****$p<0.0001$. Data are represented as mean $\pm$ SEM.
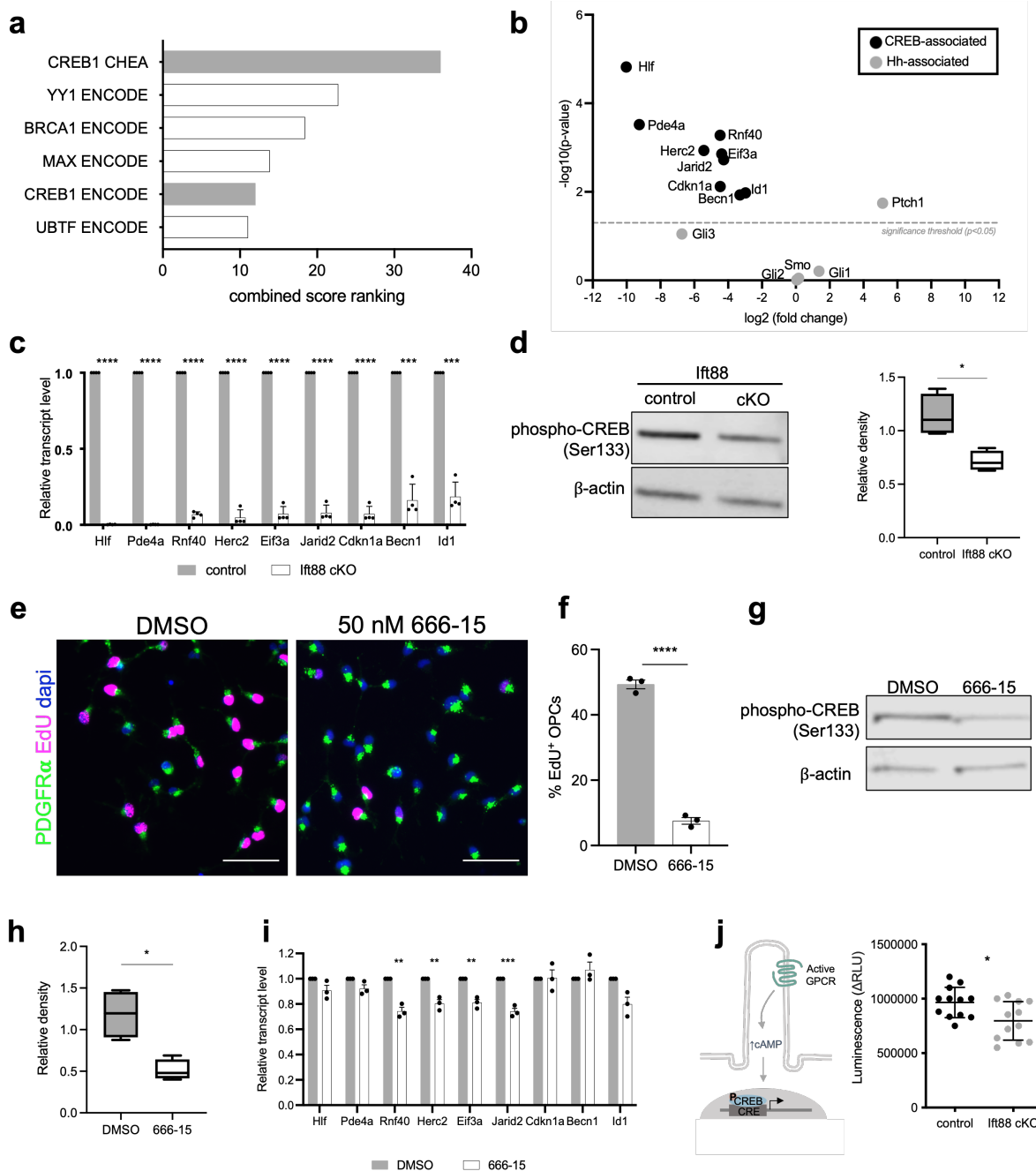
Figure 2.7. OPC cilia regulate CREB activity to promote OPC proliferation.
(a) Graphed combined score rankings from Enrichr comparing downregulated genes identified from RNA-sequencing in Ift88 cKO compared to control OPCs.
(b) CREB1-associated genes and Hh-associated genes plotted by fold-change and significance. Significance threshold set as p<0.05.
(c) qRT-PCR analysis of Ift88 cKO and control OPCs for CREB1-associated genes identified in 1b. Transcript levels in Ift88 cKO are depicted relative to controls. n=4 per genotype. Significance was determined via unpaired t-tests. A p-value less than 0.05 was considered statistically

significant, with significance denoted with the following symbols: ***p<0.001, and ****p<0.0001. Data are represented as mean $\pm$ SEM.

(d) Western blot for pCREB in control and Ift88 cKO OPCs. Quantification of western blot shows pCREB expression in Ift88 cKO relative to controls and is represented as box-and-whisker plot depicting minima, maxima, median, and interquartile range.

(e) P7 WT rat OPCs (Pdgfrα, green) treated with CREB inhibitor 666-15 and labeled with EdU (magenta).

(f) Quantification of OPCs that are EdU$^+$ in cultures treated with 50 nM 666-15 versus DMSO control, calculated by percentage of EdU$^+$Pdgfrα$^+$ cells over total Pdgfrα$^+$ cells. n=3 per condition. Significance was determined via unpaired t-test, p<0.0001. Data are represented as mean $\pm$ SEM.

(g) Western for pCREB from proteins isolated from WT OPCs treated with 50 nM 666-15 or DMSO control.

(h) Quantification of immunoblot from (g). pCREB expression in 666-15 treated OPCs is shown relative to that of DMSO treated OPCs. Data is represented as box-and-whisker plot depicting minima, maxima, median, and interquartile range. For (d) and (h), statistical significance was determined via unpaired t-test. A p-value less than 0.05 was considered statistically significant, with significance denoted with the following symbols: *p<0.05.

(i) Relative transcript levels from qRT-PCR of CREB1 associated genes identified in RNAseq studies from OPCs treated with 666-15 or DMSO, 666-15 reduces expression of CREB1 associated genes identified in RNAseq studies. Transcript levels in 666-15 cultures are depicted relative to controls. n=3 per condition. Significance was determined via unpaired t-tests. A p-value less than 0.05 was considered statistically significant, with significance denoted with the following symbols: **p<0.005 and ***p<0.001. Data are represented as mean $\pm$ SEM.

(j) cAMP levels in Ift88 cKO OPCs compared to controls assessed via cAMP Glo assay. n=12 per genotype. Unpaired t-test, p<0.05, data are represented as mean $\pm$ SEM.
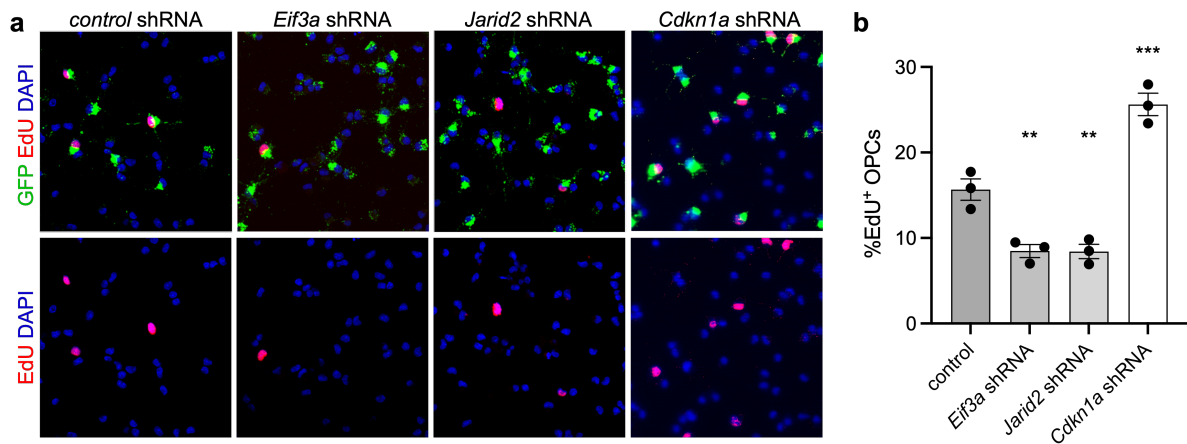
Figure 2.8. Silencing CREB1 associated genes affects OPC proliferation.
(a) OPCs from which of *Eif3a*, *Jarid2*, and *Cdkn1a* have been knocked down via shRNA in P7 WT rat OPCs (green, GFP) labeled with EdU (magenta).
(b) Quantification of (a), calculated as a percentage of EdU$^+$ OPCs. n=3. Significance was determined via one-way ANOVA followed by Dunnett's multiple comparisons test, with significance denoted with the following symbols: **$p<0.005$, ***$p<0.001$. Data are represented as mean $\pm$ SEM.

Materials and Methods

Table 2.1. Key Resource Table

REAGENT or RESOURCE	SOURCE	IDENTIFIER
Antibodies		
Rabbit anti-Arl13b	Proteintech	Cat#17711-1-AP; RRID:AB_2060867
Mouse anti-Arl13b	UC Davis/NIH Neuromab Facility	Cat# 73–287; RRID:AB_11000053
Rat anti-Pdgfrα	BD Biosciences	Cat# 558774, RRID:AB_397117
Rabbit anti-Pdgfrα	Gift from W. Stallcup	Kucharova et al., 2011[139]
Rabbit anti-Olig2	Millipore	Cat# AB9610, RRID:AB_570666
Mouse anti-Olig2	Millipore	Cat# MABN50, RRID:AB_10807410
Mouse anti-CC1	Millipore	Cat# OP80, RRID:AB_2057371
Rat anti-MBP	Bio-Rad	Cat# MCA409S, RRID:AB_325004
Chicken anti-GFP	Aves	Cat# GFP-1020, RRID:AB_10000240
Rabbit anti-GFP	Thermo Fisher	Cat# G10362, RRID:AB_2536526
Rabbit anti-cleaved caspase-3	Cell Signaling Technology	Cat# 9661, RRID:AB_2341188
Rabbit anti-phospho-CREB	Cell Signaling Technology	Cat# 9198, RRID:AB_2561044
Rabbit anti-β-actin	Proteintech	Cat# 20536-1-AP; RRID:AB_10700003
Biological samples		
Human newborn HIE tissue	UCSF Pediatric Neuropathology Research Laboratory (PNRL)	N/A
Chemicals, peptides, and recombinant proteins		
Tamoxifen	Sigma-Aldrich	Cat# T5648
Lysolecithin	Sigma-Aldrich	Cat# L4129
Human recombinant PDGF-AA	PeproTech	Cat# 100-13A
Smoothened Agonist	Milllipore	Cat# 566660
666-15	MedChemExpress	Cat# HY-101120
DMSO	Sigma-Aldrich	Cat# D8418
Critical commercial assays		
RNAeasy Mini Kit	QIAGEN	Cat# 74104
iSCRIPT cDNA Synthesis Kit	Bio-Rad	Cat# 1708891
cAMP-Glo	Promega	Cat# V1501
Experimental models: Organisms/strains		
Mouse: Ift88 fl/fl *Ift88tm1Bky*	The Jackson Laboratory	Stock No. 022409; RRID:IMSR_JAX:022409
Mouse: Pdgfrα-CreERT *Tg(Pdgfrα-Cre/ERT)467Dbe*	The Jackson Laboratory	Stock No. 018280; RRID:IMSR_JAX:018280
Mouse: Pdgfrα-Cre *Tg(Pdgfrα-Cre)1Clc/J*	The Jackson Laboratory	Stock No. 013148 RRID:IMSR_JAX:01314
Mouse: RosaEYFP (R26R-EYFP) *Gt(ROSA)26Sortm1(EYFP)Cos*	The Jackson Laboratory	Stock No. 006148; RRID:IMSR_JAX:006148

REAGENT or RESOURCE	SOURCE	IDENTIFIER
Oligonucleotides		
Ift88 flox genotyping primer F: AGGGAAGGGACTTAGGAATGA R: GACCACCTTTTTAGCCTCCTG	Integrated DNA Technologies	N/A
RosaEYFP genotyping primers WT F: CTGGCTTCTGAGGACCG WT R: CAGGACAACGCCCACACA GFP F: AGGGCGAGGAGCTGTTCA GFP R: TGAAGTCGATGCCCTTCAG	Integrated DNA Technologies	N/A
Gli1 qPCR primers F: GGTGCTGCCTATAGCCAGTGTCCTC R: GTGCCAATCCGGTGGAGTCAGACC	Integrated DNA Technologies	N/A
Ptch1 qPCR primers F: AATTCTCGACTCACTCGTCCA R: CTCCTCATATTTGGGGCCTT	Integrated DNA Technologies	N/A
Hlf qPCR primers F: GACAGCTCCCCTTGAACCC R: CTGCTGCTCTCATCGTCCA	Integrated DNA Technologies	N/A
Pde4a qPCR primers F: GAACCGGGAACTCACACACC R: GTACTCTGAGACCTGGTTTCCT	Integrated DNA Technologies	N/A
Rnf40 qPCR primers F: CACGACCACTCTAATCGAACC R: TCCAATTTCTCAATTCTCTCCCG	Integrated DNA Technologies	N/A
Herc2 qPCR primers F: CACCTGTGTATAGAGCCAAGTCA R: TTCAACCTCAAGGCTGAGAGT	Integrated DNA Technologies	N/A
Eif3a qPCR primers F: CATACAGGCAGTGTTTGGACC R: CACATAGCTTGCGGAACTCAG	Integrated DNA Technologies	N/A
Jarid2 qPCR primers F: GAAGGCGGTAAATGGGCTTCT R: TCGTTGCTAGTAGAGGACACTT	Integrated DNA Technologies	N/A
Cdkn1a qPCR primers F: CCTGGTGATGTCCGACCTG R: CCATGAGCGCATCGCAATC	Integrated DNA Technologies	N/A
Becn1 qPCR primers F: TCAGCCGGAGACTCAAGGT R: CACAGCGGGTGATCCACATC	Integrated DNA Technologies	N/A
Id1 qPCR primers F: CCTAGCTGTTCGCTGAAGGC R: CTCCGACAGACCAAGTACCAC	Integrated DNA Technologies	N/A
Gapdh qPCR primers F: ACTCCACTCACGGCAAATTC R: TCTCCATGGTGGTGAAGACA	Integrated DNA Technologies	N/A
Recombinant DNA		
pSiCoR	Gift from Tyler Jacks[140], Addgene	RRID:Addgene_11579
pSiCoR-shEif3a-EGFP target sequence: GCCTCAGTTGATGGCAAATTA	This paper	TRC clone ID: TRCN0000309153
(continued on next page)		

REAGENT or RESOURCE	SOURCE	IDENTIFIER
Recombinant DNA		
pSiCoR-shJarid2-EGFP target sequence: TGCCCAACAGTATGGTATATT	This paper	TRC clone ID: TRCN0000234444
pSiCoR-shCdkn1a-EGFP target sequence: GACCAGCCTGACAGATTTCTA	This paper	TRC clone ID: TRCN0000042584
psPAX2	Gift from Didier Trono, Addgene	RRID:Addgene_12260
pMD2.G	Gift from Didier Trono, Addgene	RRID:Addgene_12259
Software and algorithms		
GraphPad Prism 9	GraphPad Software	https://www.graphpad.com/scientific-software/prism/; RRID:SCR_015807
Fiji	Open Source	https://fiji.sc/; RRID:SCR_002285
ZEN Digital Imaging for Light Microscopy	Zeiss	RRID:SCR_013672
STAR	Dobin et al., 2013[141]	https://github.com/alexdobin/STAR/releases; RRID:SCR_004463
DESeq2	Love et al., 2014[142]	http://www.bioconductor.org/packages/release/bioc/html/DESeq2.html; RRID:SCR_015687

Experimental model and subject details

Mice

All mice were handled according to guidelines set by the University of California, San Francisco and housed within a barrier facility on a 12-hour light/dark cycle. Mice were housed with up to four other same-sex cage mates in standard rodent cages and provided food and water *ad libitum*. Both male and female mice were used for all experiments. All animal protocols and procedures were approved by UCSF's IACUC.

Pdgfrα-Cre: These mice have been described previously[143] (JAX Stock No. 013148). These mice were crossed with Ift88 floxed and RosaEYFP mice to knockout Ift88 during development, and for purification of Ift88 knockout OPCs for *in vitro* studies.

Pdgfrα-CreERT: These mice have been described previously[144] (JAX Stock No. 018280). These mice were crossed with Ift88 floxed and RosaEYFP mice. Mice were given 2 mg tamoxifen (T-5648, Sigma) dissolved in 90% corn oil/10% ethanol intraperitoneally to induce recombination.

Ift88 floxed and RosaEYFP: These mice have been described previously and were generously provided by Dr. Jeremy Reiter[145, 146] (University of California, San Francisco; Ift88 floxed previously available from JAX Stock No. 022409; RosaEYFP available from JAX Stock No. 006148). Ift88 floxed mice were crossed with Pdgfrα-Cre mice to generate constitutive Ift88 knockout in OPCs or Pdgfrα-CreERT to generate tamoxifen-inducible, conditional Ift88 knockout in OPCs. These mice were also crossed with RosaEYFP mice to report recombination. Pdgfrα-Cre: Ift88$^{fl/wt}$; RosaEYFP or Pdgfrα-CreERT: Ift88$^{fl/wt}$; RosaEYFP were crossed to Ift88$^{fl/fl}$; RosaEYFP mice to generate experimental offspring and control littermates.

Oligodendrocyte precursor cell (OPC) cultures

Primary rat or mouse OPCs were isolated from the cortical hemispheres of postnatal day 7 rat or mouse cortices (Pdgfrα-Cre: Ift88^{fl/fl} and littermate controls) as previously described[15]. Briefly, rodent cortices were minced and dissociated in papain at 37°C with periodic shaking (Worthington) for 75 min (rat) or 60 min (mouse). After trituration, the suspension was immersed in 0.2% BSA at room temperature and underwent two sequential 30 min incubations in negative selection plates (Ran-2 and Gal-C) and one 45 min incubation for positive selection of OPCs (O4). Selection plates were prepared by incubating dishes with goat IgG and IgM secondary antibodies (Jackson ImmunoResearch) in 50 mM Tris-HCl overnight at room temperature. Antibodies Ran-2, Gal-C, or O4 were added after washing with DPBS (Invitrogen). Dissociation of OPCs from positive selection dish was performed using 0.05% Trypsin-EDTA (Invitrogen) and purified OPCs were seeded onto 12mm^2 coverslips coated with poly-L-lysine (Sigma-Aldrich) at a density of 15,000 cells per coverslip. OPCs were maintained in DMEM (Invitrogen) supplemented with B27 (Invitrogen), N2 (Invitrogen), *N-acetylcysteine* (Sigma-Aldrich), forskolin (Sigma-Aldrich), penicillin-streptomycin (Invitrogen), and PDGF-AA (Peprotech) overnight at 37°C, 5% CO_2. For experiments involving SAG, purified P7 mouse Ift88 cKO and control OPCs were cultured in media containing SAG for 24 hours. OPCs were then incubated in 10 μM EdU for 2 hours to label proliferating cells. For experiments involving 666-15, purified P7 rat OPCs were cultured in media containing 50 nM 666-15 for 8 hours. OPCs were then incubated in 10 μM EdU for 2 hours to label proliferating cells.

Lysolecithin lesion

The method has been described previously[36]. Focal demyelinated lesions were produced in the white matter of the spinal cord dorsal funiculus in 10-week-old Pdgfrα-CreERT*:* Ift88^{fl/fl}; RosaEYFP and Pdgfrα-CreERT: Ift88[fl/wt]; RosaEYFP control mice after tamoxifen treatment. We used inhalational isoflurane and oxygen supplemented with subcutaneously injected 0.05 mg/kg

buprenorphine to induce and maintain anesthesia. The tissue was cleared surrounding the spinal

vertebrae at T12/T13, and the underlying spinal cord pierced with a dental needle lateral to the

midline. A Hamilton needle positioned at a 45° angle was then used to slowly inject 0.5 µl of 1%

lysolecithin through the pierced dura into the white matter of the dorsal funiculus.

Human HIE tissue

All human tissue was collected with informed consent and following guidelines established by the

Committee on Human Research at the University of California, San Francisco (H11170-19113-

07), as previously described. Immediately upon collection, brains were immersed in 4%

paraformaldehyde in PBS for 3 d. On day 3, the brain was cut coronally at the level of mammillary

body and re-immersed in fresh 4% paraformaldehyde in PBS for an additional 3 d. Tissue samples

were equilibrated in 30% sucrose in PBS for at least 2 d post-fixation then placed in molds and

embedded in optimal cutting temperature medium for 30 min at room temperatures. Samples

were then frozen in dry ice-chilled ethanol. Brain dissection and evaluation was performed by the

neuropathology staff at UCSF. HIE diagnosis requires clinical and pathological correlation; no

widely accepted diagnostic criteria are present for the pathological diagnosis of HIE.

Method details

Tamoxifen and EdU administration

Tamoxifen (T-5648, Sigma) was diluted in 90% corn oil/10% ethanol and administered

intraperitoneally in Ift88 icKO mice and littermate controls starting at 4 weeks of age. 2 mg of

tamoxifen was given to each mouse for 5 consecutive days, followed by a week of rest. The

tamoxifen injection was repeated for a total of 15 tamoxifen injections per mouse. For animal EdU

labeling experiments, EdU was diluted in a 4mg/mL stock solution in sterile 1X PBS and injected

intraperitoneally at a concentration of 40 mg/kg. For developmental studies, Ift88 cKO and control

mice were injected at P7 and at P8. For remyelination studies, Ift88 icKO and control mice were injected once at 3 dpl.

Immunohistochemistry

Mice were perfused with PBS followed by 4% (w/v) paraformaldehyde (PFA) in PBS. Brains and spinal cords were dissected and post-fixed in 4% PFA for 6 h at 4°C. After post-fixation, tissue was cryoprotected using 30% (w/v) sucrose in PBS. Tissue was sectioned at 15 μm using a cryostat (Leica CM1950). Slides with sections were stored at -80°C until use. For immunohistochemical analysis, slides were thawed at room temperature, washed 3 times with PBS and blocked in PBS containing 10% normal goat serum and 0.1% Triton X-100 for 1 h at room temperature. Primary antibodies were diluted in 10% goat serum in PBS and incubated overnight at 4°C. Slides were then incubated in goat Alexa Fluor-conjugated secondary antibodies diluted in 10% goat serum in PBS and DAPI for 1 h at room temperature. The primary antibodies used were: rabbit polyclonal anti-Arl13b (Proteintech, 17711-1-AP, 1:1000), mouse anti-Arl13b (NIH Neuromab facility, 73-287, 1:500), rabbit anti-Pdgfrα (gift from W. Stallcup), rat monoclonal anti-Pdgfrα (BD Biosciences, 558774, 1:200), mouse monoclonal anti-CC1 (Millipore, OP80, 1:500), rat monoclonal anti-MBP (Bio-Rad, MCA409S, 1:1000), chicken polyclonal anti-GFP (Aves Labs, GFP-1020, 1:1000), rabbit monoclonal anti-GFP (Thermo Fisher, G10362, 1:1000), rabbit polyclonal anti-Olig2 (Millipore, AB9610, 1:1000), mouse monoclonal anti-Olig2 (Millipore, MABN50), rabbit polyclonal anti-cleaved caspase-3 (Cell Signaling Technology, 9661, 1:500). EdU was detected in proliferating cells using the Click-iT EdU Cell Proliferation Kit for Imaging (Invitrogen C10340) according to manufacturer's instructions. Tissue sections were incubated in the reaction mix for 30 min at room temperature following secondary antibody incubation. Images were obtained on a Zeiss Axio Imager Z1 microscope. TUNEL assay was performed using the *In Situ* Cell Death Detection Kit (Roche, 12156792910).

OPC cultures were fixed in 4% (w/v) paraformaldehyde (PFA) in DPBS for 15 minutes and dehydrated. Cultures were blocked and permeabilized in 10% goat serum in DPBS containing 0.1% (v/v) Triton X-100 for 1 h at room temperature. Primary antibodies were diluted in 10% goat serum and incubated overnight at 4°C. Secondary antibodies were diluted in 10% goat serum with DAPI and incubated for 1 h at room temperature. The following primary antibodies were used: rabbit polyclonal anti-Arl13b (Proteintech, 17711-1-AP, 1:1000), rat monoclonal anti-Pdgfrα (BD Biosciences, 558774, 1:200), rabbit anti-Pdgfrα (gift from W. Stallcup), rat monoclonal anti-MBP (Bio-Rad, MCA409S, 1:1000), and chicken polyclonal anti-GFP (Aves Labs, GFP-1020, 1:1000). Alexa Fluor-conjugated secondary antibodies (rat, rabbit, 1:1000) were used to detect fluorescence. The incorporation of EdU by proliferating cells was detected via the Click-iT EdU Cell Proliferation Kit (Invitrogen C10340) after incubation in primary and secondary antibodies. Images were obtained on a Zeiss Axio Imager Z1 microscope. Cells were quantified from randomly selected fields of view per coverslip under 10x magnification.

Sample preparation for immunogold labeling

Mice were anesthetized with avertin. Fixation was performed by intracardiac perfusion with 0.9% saline solution/0.01% heparin for 5 min, followed by 15 min with 3%PFA/1% glutaraldehyde in PBS. The brain was extracted and post-fixed in the same solution overnight. Finally, brains were washed 3 times for 10 min in 1X PBS and stored in PBS/0.05% sodium azide until processing. Brains were sectioned at 50 µm using a Leica VT1000S vibratome (Leica Biosystems, Wetzlar, Germany) and sections were stored in 0.1M phosphate buffer (PB)/0.05% sodium azide.

Immunogold labeling

Tissue sections were cryoprotected in a solution containing 25% saccharose in 0.1M PB/0.05% azide for 30 min. Immediately after cryoprotection, sections were permeabilized by immersion in -60°C 2-methylbutane and rapidly transferred to a room temperature saccharose solution. This

step was repeated twice. Subsequently, tissue sections were left in 0.1M PB and then incubated in primary antibody blocking solution [0.3% BSAc (Aurion, Wageningen, The Netherlands), 0.05% sodium azide in 0.1 M PB] for 1 h. Next, the samples were incubated in primary antibody [1:200 chicken anti-GFP (Aveslab)] in primary antibody blocking solution for 72 h at 4°C. The samples were then rinsed in 0.1 M PB and incubated in secondary antibody blocking solution consisting of 0.5% BSAc (Aurion), 0.025% CWFS gelatin (Aurion), 0.05% sodium azide in 0.1 M PB for 1 h, followed by incubation in secondary antibody [1:50 goat anti-chicken IgG gold ultrasmall (Aurion)] diluted in the same secondary antibody blocking solution overnight at 4°C. To enhance gold labeling, we performed silver enhancement (R-GENT SE-LM, Aurion) for 25 min in the dark, followed by gentle washing in 2% sodium acetate and incubation in gold toning solution (0.05% gold chloride in water) for 10 min. The samples were then washed twice with 0.3% sodium thiosulfate in water. Finally, we post-fixed with 2% glutaraldehyde (Electron Microscopy Sciences) in 0.1 M PB for 30 min. Samples were rinsed and kept in 0.1 M PB containing 0.05% sodium azide at 4°C until processing them for resin embedding.

Electron microscopy processing

For transmission electron microscopy, sections were embedded in epoxy resin. First, samples were post-fixed with 1% osmium tetroxide (Electron Microscopy Sciences), 7% glucose in 0.1 M PB for 30 min at room temperature, washed in deionized water, and partially dehydrated in 70% ethanol. Afterwards, the samples were contrasted in 2% uranyl acetate (Electron Microscopy Sciences) in 70% ethanol for 2 h at 4°C. The samples were further dehydrated and embedded in Durcupan ACM epoxy resin at room temperature overnight, and then at 70°C for 72 h. Once the resin was polymerized, immunolabeled sections were selected and cut into serial semithin (1.5 μm) and then into serial ultrathin sections (60–80 nm) using an Ultracut UC7 ultramicrotome (Leica). We examined 20-25 serial ultrathin sections per cell. Ultrathin sections were placed on formvar-coated single-slot copper grids (Electron Microscopy Sciences) stained with lead citrate

and examined at 80 kV on a FEI Tecnai G2 Spirit (FEI Company, Hillsboro, OR) transmission electron microscope equipped with a Morada CCD digital camera (Olympus, Tokyo, Japan).

Quantitative RT-PCR

RNA was extracted from OPC cultures using RNeasy Mini kit (Qiagen) following manufacturer's instructions. Purified RNA was reverse transcribed to cDNA using the iScript cDNA Synthesis Kit (Bio-Rad) following manufacturer's instructions. RT-qPCR was then performed in technical triplicates with the Power SYBR Green PCR Master Mix (Applied Biosystems) and QuantStudio 3 Real-Time PCR System (Thermo Fisher). Relative expression was calculated using the ΔΔCT method normalized to *Gapdh* expression. For RT-qPCR of CREB associated genes, *Gli1* and *Ptch1* in Ift88 cKO OPCs, data were normalized to OPCs isolated from littermate control mice. For RT-qPCR of CREB-associated genes after treatment with CREB inhibitor 666-15, data were normalized to OPCs treated with DMSO. (Primers in key resources table).

Flow cytometry/Fluorescence activated cell sorting

Cells were isolated from P11 mouse cortices (control and Ift88 cKO). Briefly, mouse cortices were minced and dissociated in papain at 37°C with periodic shaking (Worthington) for 60 min. The suspension was filtered and pelleted at 1300 rpm for 5 minutes at 4°C. Pellets were resuspended in 22% Percoll (GE Healthcare) and centrifuged at 560g for 10 minutes at 4°C with no brake. After removal of myelin and debris, pelleted cells were resuspended in 2 mL of DMEM (Invitrogen) supplemented with B27 (Invitrogen), N2 (Invitrogen), *N-acetylcysteine* (Sigma-Aldrich), forskolin (Sigma-Aldrich), penicillin-streptomycin (Invitrogen), and PDGF-AA (Peprotech) and transferred to a glass tube for sorting. Cells were sorted based on EYFP fluorescence on a BD FACS Aria III and gated on forward/side scatter.

RNA-sequencing

For RNA-sequencing, a total of 3 control and 3 Ift88 cKO samples were used. For each sample, OPCs were isolated from the cortices of 4-6 mice and sorted on BD FACS Aria III flow cytometer via endogenous EYFP expression into RLT plus buffer (Qiagen). RNA was extracted and purified using a RNeasy Mini Kit (Qiagen). Libraries for RNA-seq were prepared using the QuantSeq 3' mRNA-Seq Library Prep Kit FWD (Lexogen) following manufacturer's instructions and sequenced 50-bp single-end on the HiSeq 4000 (Illumina). FastQC (http://www.bioinformatics.babraham.ac.uk/projects/fastqc) was used to assess quality of fastq files. These were aligned to the mouse reference genome GRCm38 using the STAR aligner[141]. Differential expression analysis was performed using DESeq2[142]. Pairwise comparisons were performed between control and Ift88 knockout OPCs. Genes were selected by a significance threshold of $p<0.05$, log2FC>1 or log2FC<-1.

SDS-PAGE and western blotting

OPCs were purified from rat or mouse cortices. Cells were lysed in ice-cold RIPA buffer containing protease inhibitor, agitated for 30 min at 4°C, and sonicated 3 times for 10 sec. The sample was centrifuged at 16000 x g for 20 min at 4°C and pellet discarded. Protein concentrations were determined using BCA protein assay kit (Thermo Fisher). Samples were run on 10% precast TGX gels (Bio-Rad) and transferred to PVDF membranes, blocked with 3% BSA in TBS-T for 1 hour at room temperature, incubated with rabbit monoclonal anti-phosphorylated CREB antibody (Cell Signaling Technology, 9198, 1:1000) or rabbit polyclonal anti-β-actin antibody (Proteintech, 20536-1-AP, 1:1000) at 4°C overnight, followed by washes and secondary antibody (LICOR IRDye, 1:2000) at room temperature for 1 h. Images were acquired on a Li-Cor Odyssey scanner.

cAMP Measurements

To assess cAMP levels in Ift88 cKO OPCs and controls, we used the cAMP-Glo kit (Promega). OPCs were seeded into 12-well plates at a density of 50,000 cells per well in media containing PDGF-AA as described above. PDGF-AA was then removed from media for 4 hours and incubated in cAMP-Glo Lysis Buffer and transferred to 96 well plates. cAMP-Glo assay was performed according to manufacturer's instructions, and plates were read using a microplate reader luminometer.

shRNA and lentiviral transduction

shRNAs were cloned in pSiCoR vectors (Addgene, 11579). For the generation of lentivirus containing shRNA vectors, lentivirus was produced in HEK293FT cells. HEK293FT cells were co-transfected with the appropriate lentiviral vector and packaging plasmids psPAX2 and pMD2.G at a 0.50:025:0.25 ratio using polyethylenimine (PEI) at a 1:3 DNA:PEI ratio. Cells were initially cultured in DMEM containing 10% FBS for 24 h, after which the media was changed to OPC culture media as described above. The viral supernatant was collected at 48 h post-transfection, filtered, and used for infection of OPCs with Polybrene reagent (EMD Millipore, 1:500).

Quantifications and statistical analysis

Quantifications

All images were acquired on a Zeiss Axio Imager Z1 microscope. For quantifications in OPC cultures, cells were quantified from eight randomly selected fields of view per coverslip under 10x magnification. Sample size (n) for cell culture experiments indicates number of independent experiments. For quantifications of cells in the mouse cortex, two fields were manually quantified per section in Fiji, using three averaged sections per mice. Sections were anatomically matched across mice. For density quantifications in dorsal funiculus spinal cord lesions, the number of EYFP$^+$ cells were divided by the area of the lesion per section. This value was averaged across

three lesioned spinal cord sections per mice. Sample size (n) for animal experiments indicates number of mice used per experiment. Each individual data point represents average values per mouse. All image quantifications were conducted blinded.

Statistical analysis

Statistical analyses and graphing were performed using GraphPad Prism 9 software. We used unpaired t-tests to determine the statistical significance between two experimental groups (between genotypes or treatment conditions). For more than two samples, significance was determined via one-way ANOVA with Dunnett's post-hoc analysis or two-way ANOVA with Tukey's post-hoc analysis for two variables. For dot plots and bar graphs, data are presented as mean $\pm$ SEM. For box-and-whisker plots, the center represents the median while the box represents the interquartile range with whiskers indicating minimum and maximum values. A threshold of $p < 0.05$ was considered statistically significant. Statistical significance is denoted with the following symbols: ns indicates not significant, $*p < 0.05$, $**p < 0.01$, $***p < 0.001$, and $****p < 0.0001$.

Chapter 3: Conclusions and Future Directions

Conclusion

In this work, we have characterized the dynamic nature of OPC ciliation *in vitro* and *in vivo* across different time points, suggesting that OPCs can be receptive to signals transduced through primary cilia throughout life (**Figure 2.1**). Our functional studies, where we remove Ift88 to disrupt ciliogenesis, identify the primary cilium as a critical signaling organelle regulating OPC proliferation during CNS development and WMI repair (**Figure 2.2, 2.5**). This discovery prompted us to establish the mechanism by which cilia are involved in OPC proliferation. We first hypothesized that OPC cilia transduce Hh signals based on the literature showing that (1) defects in ciliary machinery result in dysregulated Hh transduction in many cell types[67, 72, 73, 90, 92, 115] and (2) OPCs can transduce Hh signals after specification[96, 98]. However, we found that the expression of Hedgehog target genes is not significantly altered in OPC cilia knockout mice (Ift88 cKO) compared to their controls. Additionally, OPCs that lost cilia proliferated in response to Smoothened agonist, suggesting that OPCs do not require primary cilia for Hh signal transduction (**Figure 2.6**). We then moved to an unbiased approach of identifying signaling mechanisms altered by loss of cilia. Our transcriptional analysis of OPCs from Ift88 cKO mice compared to controls reveals a significant downregulation in genes that are associated with cAMP response element binding protein (CREB) binding sites. As CREB lies downstream of cAMP and GPCRs, this finding led us to investigate CREB activity in Ift88 cKO OPCs. Altogether, we identify that signaling through OPC primary cilia is required for CREB activation and the transcription of genes that regulate OPC proliferation (**Figure 2.7**). This work provides a platform from which new cilia-specific signaling pathways can be identified in the control OPC biology, which may inform future strategies for promoting remyelination.

Future Directions

This study, along with its limitations, raises several new questions. Does the reduction in OPC proliferation translate to reduced myelination in the developing CNS and reduced

regeneration of myelin in WMI repair? Even though OPCs don't require primary cilia to transduce Hh signals, can OPC cilia transduce these signals? What signaling molecules and effectors lie upstream of cAMP/CREB to control OPC proliferation? I explore these questions and propose ways to answer them in the following paragraphs.

Our results indicate that ciliary control of proliferation contributes to the decreased EYFP$^+$ OPCs generated in the Ift88 cKO. Interestingly, the number of total Pdgfrα$^+$ OPCs in the developing cortex remains unchanged in Ift88 cKO compared to controls. We found that EYFP$^-$ Pdgfrα$^+$ OPCs compensated for the reduction in EYFP$^+$Pdgfrα$^+$ OPCs via hyperproliferation (**Figure 2.3a-b**). These data are consistent with studies showing that OPCs undergo a proliferative burst to quickly restore density after the loss of neighboring OPCs[113]. This presents one limitation of our study, as the regenerative capacity of OPCs from cells that escaped recombination precludes our ability to fully assess how the failed expansion of EYFP$^+$ OPCs affects the entire remyelination process. It would be interesting to determine whether the impairment of OPC proliferation due to loss of cilia contributes to reduced myelin formation within lesions. To achieve this might require a modified tamoxifen injection paradigm, where recombination is induced continuously prior to and after surgery to reduce the presence of cells escaping recombination. To track recombined OPCs that differentiate into myelin forming OLs, it would be best to use a membrane-localized reporter (e.g., mGFP) that can be visualized in myelin.

One of the surprising outcomes of this work was the finding that primary cilia are not required for Hh signal transduction in OPCs. There is evidence for Smo signaling competency in the absence of Smo ciliary accumulation[131], suggesting that the OPC response to SAG in the absence of primary cilia occurs through extraciliary Smo activation (**Figure 2.6**). However, what our results do not address is how Smo accumulates in the absence of cilia or whether Smo accumulates in OPC cilia when they are present. The only conclusion we can draw from these data is that Hh signaling in OPCs does not require cilia and is not the mechanism underlying the proliferation deficit observed in OPC cilia knockout mice. Further studies on the dynamics of Smo

accumulation and localization in WT OPCs cultured with SAG might provide insights as to whether OPC cilia are able to promote Hh signal transduction, or if in OPCs all Hh signaling occurs outside of the cilium regardless of its presence.

The biggest question that arises from this work is: what ciliary localized components lie upstream of cAMP and CREB that function to promote OPC proliferation? We hypothesize, based on the involvement of cAMP and evidence of cilia being centers for GPCR signal transduction, that this signaling is initiated at a ciliary GPCR. Functionally relevant GPCRs expressed in OPCs include Gpr56 and Gpr17[100, 101]. There is no evidence that these GPCRs function through mediating CREB activity, so it is unclear whether these are the GPCRs responsible for the phenotypes observed in our study. However, it would be interesting to determine whether they localize to cilia. This would require overexpressing GFP-tagged versions of these GPCRs in OPCs. While a model of there being a single ciliary GPCR responsible for the OPC proliferation deficits demonstrated here would be convenient, it is highly unlikely as multiple GPCRs, pathway effectors, and even other types of receptors may localize and interact within OPC cilia to create a specific intracellular response. The unbiased and comprehensive identification of proteins that survey OPC cilia through proteomics profiling[106, 107] will reveal a list of signaling molecules that may be required for proper OPC function as well as ciliary GPCRs that may be the upstream effectors of cAMP and CREB activity in OPCs.

Initial proteomics studies of OPC primary cilia

In 2015, the lab of Maxence Nachury developed a proximity labeling approach to study the ciliary proteome[106] using APEX2, an enzyme that biotinylates proteins in the presence of hydrogen peroxide (H_2O_2). Briefly, APEX2 catalyzes the oxidation of biotin-phenol into a biotin-phenoxyl radical that subsequently reacts with amino acids on neighboring proteins, resulting in their biotinylation. A small portion of proteins that localize to cilia contain defined ciliary targeting sequences (CTS) – motifs that target proteins to the ciliary axoneme. APEX2 was fused to the

CTS of ciliary NPHP3 to guide APEX2 localization to primary cilia (cilia-APEX). With APEX2 targeted to cilia, ciliary proteins can be directly biotinylated, purified, and identified through mass spectrometry (**Figure 3.1**). The original cilia-APEX2 study identified known ciliary localized proteins, such as Ift88 and Arl13B. Candidates also included new, unexpected signaling proteins, and detected GPCRs such as Gpr161[106]. Furthermore, cilia-APEX has been used to study the dynamic nature of the ciliary proteome, resolving time-dependent changes in the context of Hedgehog signaling[107]. These studies establish cilia-APEX as a useful tool in studying novel ciliary constituents alongside signaling components.

We have applied cilia-APEX to OPCs in preliminary studies to try to define the proteome of the OPC primary cilium. We adapted the cilia-APEX and control-APEX constructs from the Nachury lab. As OPCs are notoriously difficult to transfect with high efficiency, we sub-cloned these constructs into a lentiviral vector and produced lentiviruses to transduce purified primary mouse OPCs *in vitro*. Localization of Alexa Fluor 647-labeled streptavidin (SA647) to the primary cilium in OPCs with cilia-APEX suggests that incubation of OPCs with biotin-phenol and H_2O_2 results in efficient and selective biotinylation of ciliary proteins (**Figure 3.2**). Next, we conducted preliminary mass spectrometry analyses (liquid chromatography/MS-MS) of the cilia-APEX-labeled samples (in collaboration with Ruth Huttenhain[147]). We analyzed unlabeled cilia-APEX (cilia-APEX without biotin) and labeled control-APEX samples to control for the contribution of endogenously biotinylated proteins and non-ciliary APEX biotinylated proteins, respectively. We selected proteins that were enriched 1.5-fold in intensity (estimated intensity per protein based on individual peptide measurements) compared to the controls. We identified 129 proteins enriched in the labeled cilia-APEX samples compared to controls, and 25 potential candidate ciliary proteins that were present in the labeled cilia-APEX samples only (**Figure 3.3a**). Several of these identified proteins have previously reported associations to primary cilia, demonstrating the feasibility of proteomic profiling of primary cilia in OPCs (**Figure 3.3b**).

While we could identify some proteins localized to the OPC primary cilium, many of the common ciliary localized proteins, such as Arl13b, were missing from our analysis. This is possibly due to the displacement of endogenous ciliary proteins caused by attempts to achieve high efficiency of cilia-APEX expression in our *in vitro* overexpression system. The development of new proximity labeling techniques for proteomic profiling of the primary cilium in a broad range of cell types is therefore needed to uncover additional ciliary GPCRs and ciliary signaling molecules in general.

As evidenced by the well-resolved model of Hh signal transduction through primary cilia[107], the ciliary proteome has the potential to be highly dynamic in response to surrounding cues. Once the appropriate tools are established, we can better understand the dynamics of the proteins that survey OPC cilia in different contexts. For example, does the content of OPC primary cilia change across different time points during development in response to the changing microenvironment? Do the microenvironmental signals present during WMI repair affect the proteome of OPC cilia? Through the comparison of ciliary constituents in these distinct contexts, we will identify potential differences in how primary cilia regulate OPC biology across different stages. This can inform new therapeutic strategies that could be effective in disorders involving dysfunctional myelination.
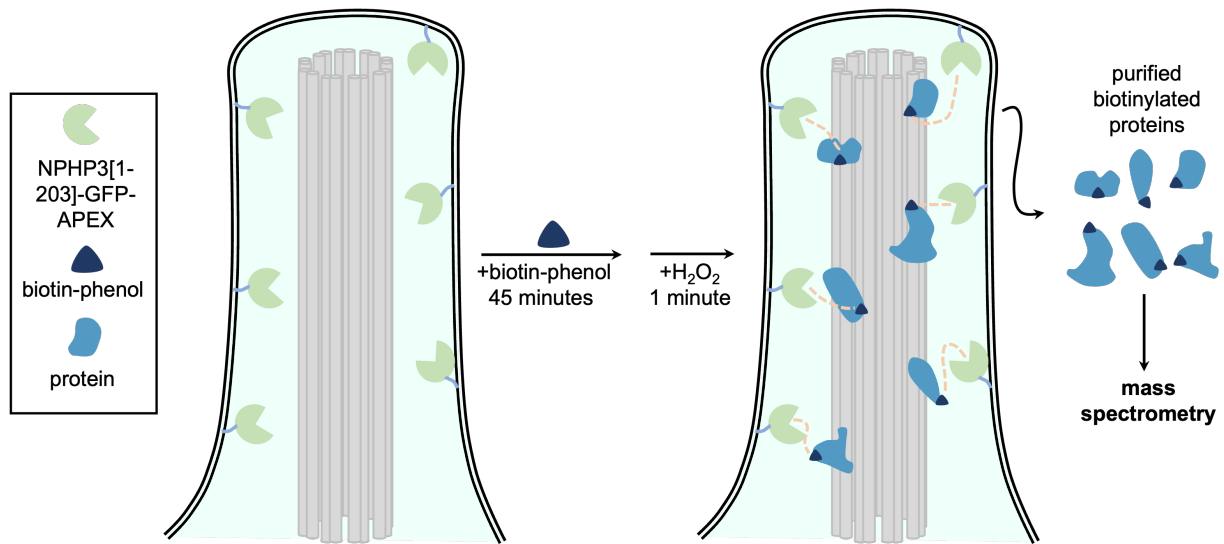
Figure 3.1. Diagram of proximity labeling method in cilia[106].
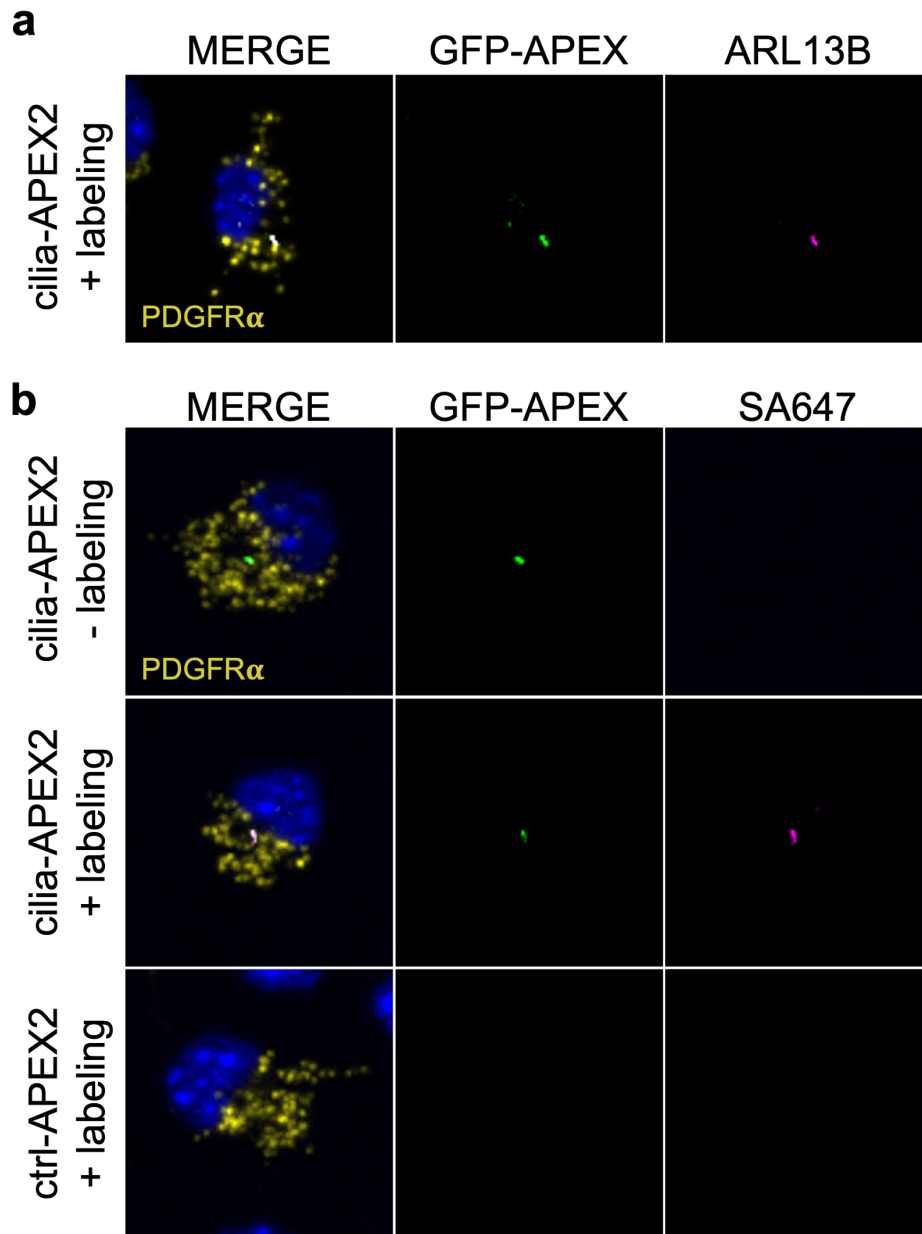
Figure 3.2. Cilia-APEX2 biotinylates ciliary proteins in OPCs.
(a) OPCs *in vitro* expressing cilia-APEX2 (GFP, green) in primary cilia (Arl13b, magenta).
(b) Biotinylated ciliary proteins (SA647, magenta) in OPCs (Pdgfrα, yellow) expressing cilia-APEX2 (GFP, green) after labeling with biotin-phenol and H_2O_2.

a cilia-APEX + labeling

25

28   51

25

26   33   6

cilia-APEX -
labeling

control-APEX +
labeling

b

Ciliary structure
Dpysl2
Septins
Sept7
Sept8
MT-associated
Tubb2a
Tubb3

Ubiquitin
Uba1
Cand1

Ciliary trafficking
Gdi2
Ran; Rasl2-9

Ciliary signaling
Phosphatase
Ppp2r1a

Figure 3.3. Ciliary proteins from mass spectrometry analysis of cilia-APEX2 in primary OPCs.
(a) Venn diagram of proteins identified after streptavidin chromatography. Numbers highlighted in yellow represent proteins enriched at least 1.5-fold in cilia-APEX2 samples compared to both controls. Bold number represents number of candidate ciliary proteins.
(b) Candidate ciliary proteins grouped into functional categories.

Materials and Methods

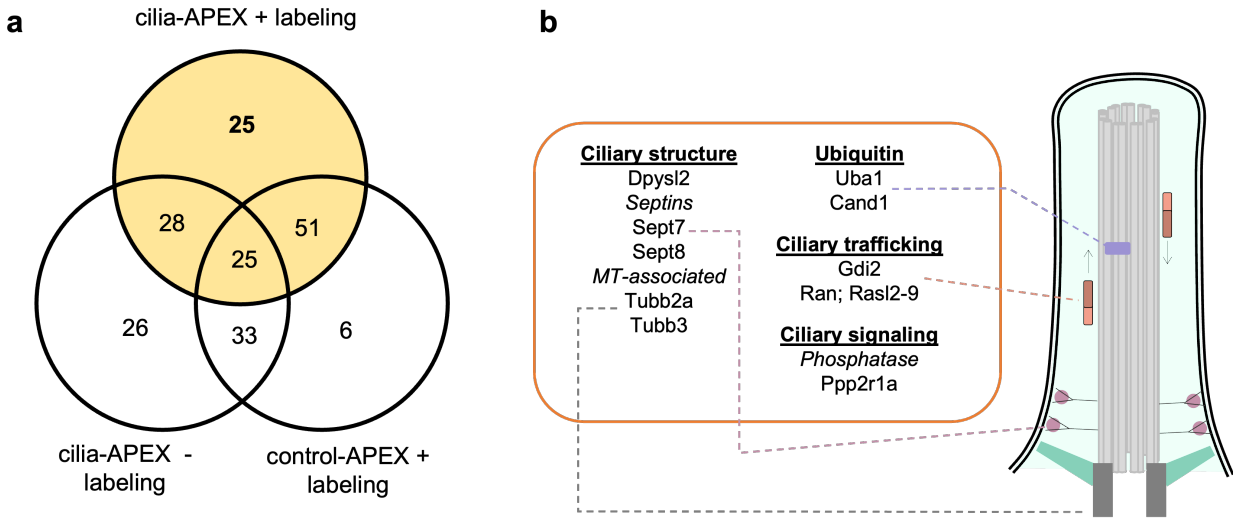**Oligodendrocyte precursor cell (OPC) cultures**

Primary mouse OPCs were isolated from the cortical hemispheres of postnatal day 7 mouse brains as previously described[15]. Briefly, mouse cortices were minced and dissociated in papain at 37°C with periodic shaking (Worthington) for 60 min. After trituration, the suspension was immersed in 0.2% BSA at room temperature and underwent two sequential 30 min incubations in negative selection plates (Ran-2 and Gal-C) and one 45 min incubation for positive selection of OPCs (O4). Selection plates were prepared by incubating dishes with goat IgG and IgM secondary antibodies (Jackson ImmunoResearch) in 50 mM Tris-HCl overnight at room temperature. Antibodies Ran-2, Gal-C, or O4 were added after washing with DPBS (Invitrogen). Dissociation of OPCs from positive selection dish was performed using 0.05% Trypsin-EDTA (Invitrogen) and purified OPCs were seeded onto 12mm^2 coverslips coated with poly-L-lysine (Sigma-Aldrich) at a density of 15,000 cells per coverslip. OPCs were maintained in DMEM (Invitrogen) supplemented with B27 (Invitrogen), N2 (Invitrogen), *N-acetylcysteine* (Sigma-Aldrich), forskolin (Sigma-Aldrich), penicillin-streptomycin (Invitrogen), and PDGF-AA (Peprotech) overnight at 37°C, 5% CO_2.

Lentiviral transduction

Cilia-APEX and control-APEX constructs (Addgene, 73186 and 73187) were subcloned into pCDH vectors. For the generation of lentivirus containing control-APEX and cilia-APEX, lentivirus was produced in HEK293FT cells. HEK293FT cells were co-transfected with the appropriate lentiviral vector and packaging plasmids psPAX2 and pMD2.G at a 0.50:025:0.25 ratio using polyethylenimine (PEI) at a 1:3 DNA:PEI ratio. Cells were initially cultured in DMEM containing 10% FBS for 24 h, after which the media was changed to OPC culture media as described above. The viral supernatant was collected at 48 h post-transfection, filtered, and used for infection of OPCs with Polybrene reagent (EMD Millipore, 1:500).

APEX labeling

After lentiviral infection, OPCs were cultured in media containing PDGF-AA to recover. They were then incubated in media without PDGF-AA to halt OPC proliferation and induce ciliation *in vitro*. In this media, OPCs were incubated in the presence of 0.5 mM biotin-phenol for 45 min, followed by 1 mM H_2O_2 for 1 min to catalyze protein biotinylation. Cells were then washed with quenching buffer (PBS, 10 mM sodium ascorbate, 10 mM sodium azide, 5 mM Trolox). OPCs were then fixed for imaging or lysed for mass spectrometry analysis.

Streptavidin chromatography

Cilia-APEX and control-APEX expressing OPCs were lysed in ice-cold RIPA buffer containing protease inhibitor, agitated for 30 min at 4°C, and sonicated 3 times for 10 sec. The sample was centrifuged at 16000 x g for 20 min at 4°C and pellet discarded. Protein concentrations were determined using BCA protein assay kit (Thermo Fisher). The supernatant was then diluted and loaded onto streptavidin-agarose beads to purify biotinylated proteins (Thermo Scientific, 20349). Lysate and beads were mixed for 1 h at room temperature, after which beads were washed with wash buffer. Biotinylated proteins were eluted by boiling beads in SDS sample buffer supplemented with 2 mM biotin.

Immunohistochemistry

OPC cultures were fixed in 4% (w/v) paraformaldehyde (PFA) in DPBS for 15 minutes and dehydrated. Cultures were blocked and permeabilized in 10% goat serum in DPBS containing 0.1% (v/v) Triton X-100 for 1 h at room temperature. Primary antibodies were diluted in 10% goat serum and incubated overnight at 4°C. Secondary antibodies were diluted in 10% goat serum with DAPI and incubated for 1 h at room temperature. The following primary antibodies were used: rabbit polyclonal anti-Arl13b (Proteintech, 17711-1-AP, 1:1000), rat monoclonal anti-Pdgfrα (BD Biosciences, 558774, 1:200). Alexa Fluor-conjugated secondary antibodies (rat, rabbit, 1:1000)

and IRDye 680 RD streptavidin (Licor) were used to detect fluorescence. Images were obtained on a Zeiss Axio Imager Z1 microscope.

References

(1) Walton, C.; King, R.; Rechtman, L.; Kaye, W.; Leray, E.; Marrie, R. A.; Robertson, N.; La Rocca, N.; Uitdehaag, B.; van der Mei, I.; et al. Rising prevalence of multiple sclerosis worldwide: Insights from the Atlas of MS, third edition. *Mult Scler* **2020**, *26* (14), 1816-1821. DOI: 10.1177/1352458520970841.

(2) Reich, D. S.; Lucchinetti, C. F.; Calabresi, P. A. Multiple Sclerosis. *N Engl J Med* **2018**, *378* (2), 169-180. DOI: 10.1056/NEJMra1401483.

(3) Thompson, A. J.; Baranzini, S. E.; Geurts, J.; Hemmer, B.; Ciccarelli, O. Multiple sclerosis. *Lancet* **2018**, *391* (10130), 1622-1636. DOI: 10.1016/S0140-6736(18)30481-1.

(4) Lublin, F. D.; Reingold, S. C. Defining the clinical course of multiple sclerosis: results of an international survey. National Multiple Sclerosis Society (USA) Advisory Committee on Clinical Trials of New Agents in Multiple Sclerosis. *Neurology* **1996**, *46* (4), 907-911. DOI: 10.1212/wnl.46.4.907.

(5) Lublin, F. D.; Reingold, S. C.; Cohen, J. A.; Cutter, G. R.; Sørensen, P. S.; Thompson, A. J.; Wolinsky, J. S.; Balcer, L. J.; Banwell, B.; Barkhof, F.; et al. Defining the clinical course of multiple sclerosis: the 2013 revisions. *Neurology* **2014**, *83* (3), 278-286. DOI: 10.1212/WNL.0000000000000560.

(6) Cree, B. A.; Gourraud, P. A.; Oksenberg, J. R.; Bevan, C.; Crabtree-Hartman, E.; Gelfand, J. M.; Goodin, D. S.; Graves, J.; Green, A. J.; Mowry, E.; et al. Long-term evolution of multiple sclerosis disability in the treatment era. *Ann Neurol* **2016**, *80* (4), 499-510. DOI: 10.1002/ana.24747.

(7) Lunde, H. M. B.; Assmus, J.; Myhr, K. M.; Bø, L.; Grytten, N. Survival and cause of death in multiple sclerosis: a 60-year longitudinal population study. *J Neurol Neurosurg Psychiatry* **2017**, *88* (8), 621-625. DOI: 10.1136/jnnp-2016-315238.

(8) Bierhansl, L.; Hartung, H. P.; Aktas, O.; Ruck, T.; Roden, M.; Meuth, S. G. Thinking outside the box: non-canonical targets in multiple sclerosis. *Nat Rev Drug Discov* **2022**, *21* (8), 578-600. DOI: 10.1038/s41573-022-00477-5.

(9) Voge, N. V.; Alvarez, E. Monoclonal Antibodies in Multiple Sclerosis: Present and Future. *Biomedicines* **2019**, *7* (1). DOI: 10.3390/biomedicines7010020.

(10) Montalban, X.; Hauser, S. L.; Kappos, L.; Arnold, D. L.; Bar-Or, A.; Comi, G.; de Seze, J.; Giovannoni, G.; Hartung, H. P.; Hemmer, B.; et al. Ocrelizumab versus Placebo in Primary Progressive Multiple Sclerosis. *N Engl J Med* **2017**, *376* (3), 209-220. DOI: 10.1056/NEJMoa1606468.

(11) Franklin, R. J. M.; Simons, M. CNS remyelination and inflammation: From basic mechanisms to therapeutic opportunities. *Neuron* **2022**, *110* (21), 3549-3565. DOI: 10.1016/j.neuron.2022.09.023.

(12) Zawadzka, M.; Rivers, L. E.; Fancy, S. P.; Zhao, C.; Tripathi, R.; Jamen, F.; Young, K.; Goncharevich, A.; Pohl, H.; Rizzi, M.; et al. CNS-resident glial progenitor/stem cells produce Schwann cells as well as oligodendrocytes during repair of CNS demyelination. *Cell Stem Cell* **2010**, *6* (6), 578-590. DOI: 10.1016/j.stem.2010.04.002.

(13) Bacmeister, C. M.; Barr, H. J.; McClain, C. R.; Thornton, M. A.; Nettles, D.; Welle, C. G.; Hughes, E. G. Motor learning promotes remyelination via new and surviving oligodendrocytes. *Nat Neurosci* **2020**, *23* (7), 819-831. DOI: 10.1038/s41593-020-0637-3.

(14) Neely, S. A.; Williamson, J. M.; Klingseisen, A.; Zoupi, L.; Early, J. J.; Williams, A.; Lyons, D. A. New oligodendrocytes exhibit more abundant and accurate myelin regeneration than those that survive demyelination. *Nat Neurosci* **2022**, *25* (4), 415-420. DOI: 10.1038/s41593-021-01009-x.

(15) Mei, F.; Fancy, S. P. J.; Shen, Y. A.; Niu, J.; Zhao, C.; Presley, B.; Miao, E.; Lee, S.; Mayoral, S. R.; Redmond, S. A.; et al. Micropillar arrays as a high-throughput screening platform

for therapeutics in multiple sclerosis. *Nat Med* **2014**, *20* (8), 954-960. DOI: 10.1038/nm.3618.

(16) Cree, B. A. C.; Niu, J.; Hoi, K. K.; Zhao, C.; Caganap, S. D.; Henry, R. G.; Dao, D. Q.; Zollinger, D. R.; Mei, F.; Shen, Y. A.; et al. Clemastine rescues myelination defects and promotes functional recovery in hypoxic brain injury. *Brain* **2018**, *141* (1), 85-98. DOI: 10.1093/brain/awx312.

(17) Mei, F.; Mayoral, S. R.; Nobuta, H.; Wang, F.; Desponts, C.; Lorrain, D. S.; Xiao, L.; Green, A. J.; Rowitch, D.; Whistler, J.; et al. Identification of the Kappa-Opioid Receptor as a Therapeutic Target for Oligodendrocyte Remyelination. *J Neurosci* **2016**, *36* (30), 7925-7935. DOI: 10.1523/JNEUROSCI.1493-16.2016.

(18) Lucchinetti, C.; Brück, W.; Parisi, J.; Scheithauer, B.; Rodriguez, M.; Lassmann, H. A quantitative analysis of oligodendrocytes in multiple sclerosis lesions. A study of 113 cases. *Brain* **1999**, *122 (Pt 12)*, 2279-2295. DOI: 10.1093/brain/122.12.2279.

(19) Boyd, A.; Zhang, H.; Williams, A. Insufficient OPC migration into demyelinated lesions is a cause of poor remyelination in MS and mouse models. *Acta Neuropathol* **2013**, *125* (6), 841-859. DOI: 10.1007/s00401-013-1112-y.

(20) Richardson, W. D.; Kessaris, N.; Pringle, N. Oligodendrocyte wars. *Nat Rev Neurosci* **2006**, *7* (1), 11-18. DOI: 10.1038/nrn1826.

(21) Bergles, D. E.; Richardson, W. D. Oligodendrocyte Development and Plasticity. *Cold Spring Harb Perspect Biol* **2015**, *8* (2), a020453. DOI: 10.1101/cshperspect.a020453.

(22) Warf, B. C.; Fok-Seang, J.; Miller, R. H. Evidence for the ventral origin of oligodendrocyte precursors in the rat spinal cord. *J Neurosci* **1991**, *11* (8), 2477-2488. DOI: 10.1523/JNEUROSCI.11-08-02477.1991.

(23) Cai, J.; Qi, Y.; Hu, X.; Tan, M.; Liu, Z.; Zhang, J.; Li, Q.; Sander, M.; Qiu, M. Generation of oligodendrocyte precursor cells from mouse dorsal spinal cord independent of Nkx6

regulation and Shh signaling. *Neuron* **2005**, *45* (1), 41-53. DOI: 10.1016/j.neuron.2004.12.028.

(24) Fogarty, M.; Richardson, W. D.; Kessaris, N. A subset of oligodendrocytes generated from radial glia in the dorsal spinal cord. *Development* **2005**, *132* (8), 1951-1959. DOI: 10.1242/dev.01777.

(25) Vallstedt, A.; Klos, J. M.; Ericson, J. Multiple dorsoventral origins of oligodendrocyte generation in the spinal cord and hindbrain. *Neuron* **2005**, *45* (1), 55-67. DOI: 10.1016/j.neuron.2004.12.026.

(26) Kessaris, N.; Fogarty, M.; Iannarelli, P.; Grist, M.; Wegner, M.; Richardson, W. D. Competing waves of oligodendrocytes in the forebrain and postnatal elimination of an embryonic lineage. *Nat Neurosci* **2006**, *9* (2), 173-179. DOI: 10.1038/nn1620.

(27) Briscoe, J.; Ericson, J. Specification of neuronal fates in the ventral neural tube. *Curr Opin Neurobiol* **2001**, *11* (1), 43-49. DOI: 10.1016/s0959-4388(00)00172-0.

(28) Li, H.; de Faria, J. P.; Andrew, P.; Nitarska, J.; Richardson, W. D. Phosphorylation regulates OLIG2 cofactor choice and the motor neuron-oligodendrocyte fate switch. *Neuron* **2011**, *69* (5), 918-929. DOI: 10.1016/j.neuron.2011.01.030.

(29) Orentas, D. M.; Hayes, J. E.; Dyer, K. L.; Miller, R. H. Sonic hedgehog signaling is required during the appearance of spinal cord oligodendrocyte precursors. *Development* **1999**, *126* (11), 2419-2429. DOI: 10.1242/dev.126.11.2419.

(30) Alberta, J. A.; Park, S. K.; Mora, J.; Yuk, D.; Pawlitzky, I.; Iannarelli, P.; Vartanian, T.; Stiles, C. D.; Rowitch, D. H. Sonic hedgehog is required during an early phase of oligodendrocyte development in mammalian brain. *Mol Cell Neurosci* **2001**, *18* (4), 434-441. DOI: 10.1006/mcne.2001.1026.

(31) Nery, S.; Wichterle, H.; Fishell, G. Sonic hedgehog contributes to oligodendrocyte specification in the mammalian forebrain. *Development* **2001**, *128* (4), 527-540. DOI: 10.1242/dev.128.4.527.

(32) Tekki-Kessaris, N.; Woodruff, R.; Hall, A. C.; Gaffield, W.; Kimura, S.; Stiles, C. D.; Rowitch, D. H.; Richardson, W. D. Hedgehog-dependent oligodendrocyte lineage specification in the telencephalon. *Development* **2001**, *128* (13), 2545-2554. DOI: 10.1242/dev.128.13.2545.

(33) Winkler, C. C.; Yabut, O. R.; Fregoso, S. P.; Gomez, H. G.; Dwyer, B. E.; Pleasure, S. J.; Franco, S. J. The Dorsal Wave of Neocortical Oligodendrogenesis Begins Embryonically and Requires Multiple Sources of Sonic Hedgehog. *J Neurosci* **2018**, *38* (23), 5237-5250. DOI: 10.1523/JNEUROSCI.3392-17.2018.

(34) Paredes, I.; Vieira, J. R.; Shah, B.; Ramunno, C. F.; Dyckow, J.; Adler, H.; Richter, M.; Schermann, G.; Giannakouri, E.; Schirmer, L.; et al. Oligodendrocyte precursor cell specification is regulated by bidirectional neural progenitor-endothelial cell crosstalk. *Nat Neurosci* **2021**, *24* (4), 478-488. DOI: 10.1038/s41593-020-00788-z.

(35) Tsai, H. H.; Niu, J.; Munji, R.; Davalos, D.; Chang, J.; Zhang, H.; Tien, A. C.; Kuo, C. J.; Chan, J. R.; Daneman, R.; et al. Oligodendrocyte precursors migrate along vasculature in the developing nervous system. *Science* **2016**, *351* (6271), 379-384. DOI: 10.1126/science.aad3839.

(36) Niu, J.; Tsai, H. H.; Hoi, K. K.; Huang, N.; Yu, G.; Kim, K.; Baranzini, S. E.; Xiao, L.; Chan, J. R.; Fancy, S. P. J. Aberrant oligodendroglial-vascular interactions disrupt the blood-brain barrier, triggering CNS inflammation. *Nat Neurosci* **2019**, *22* (5), 709-718. DOI: 10.1038/s41593-019-0369-4.

(37) Fruttiger, M.; Karlsson, L.; Hall, A. C.; Abramsson, A.; Calver, A. R.; Boström, H.; Willetts, K.; Bertold, C. H.; Heath, J. K.; Betsholtz, C.; et al. Defective oligodendrocyte development and severe hypomyelination in PDGF-A knockout mice. *Development* **1999**, *126* (3), 457-467. DOI: 10.1242/dev.126.3.457.

(38) Richardson, W. D.; Pringle, N.; Mosley, M. J.; Westermark, B.; Dubois-Dalcq, M. A role for platelet-derived growth factor in normal gliogenesis in the central nervous system. *Cell* **1988**, *53* (2), 309-319.

(39) Robinson, S.; Tani, M.; Strieter, R. M.; Ransohoff, R. M.; Miller, R. H. The chemokine growth-regulated oncogene-alpha promotes spinal cord oligodendrocyte precursor proliferation. *J Neurosci* **1998**, *18* (24), 10457-10463.

(40) Redwine, J. M.; Armstrong, R. C. In vivo proliferation of oligodendrocyte progenitors expressing PDGFalphaR during early remyelination. *J Neurobiol* **1998**, *37* (3), 413-428.

(41) Noble, M.; Murray, K.; Stroobant, P.; Waterfield, M. D.; Riddle, P. Platelet-derived growth factor promotes division and motility and inhibits premature differentiation of the oligodendrocyte/type-2 astrocyte progenitor cell. *Nature* **1988**, *333* (6173), 560-562. DOI: 10.1038/333560a0.

(42) Calver, A. R.; Hall, A. C.; Yu, W. P.; Walsh, F. S.; Heath, J. K.; Betsholtz, C.; Richardson, W. D. Oligodendrocyte population dynamics and the role of PDGF in vivo. *Neuron* **1998**, *20* (5), 869-882.

(43) Woodruff, R. H.; Fruttiger, M.; Richardson, W. D.; Franklin, R. J. Platelet-derived growth factor regulates oligodendrocyte progenitor numbers in adult CNS and their response following CNS demyelination. *Mol Cell Neurosci* **2004**, *25* (2), 252-262. DOI: 10.1016/j.mcn.2003.10.014.

(44) Tsai, H. H.; Tessier-Lavigne, M.; Miller, R. H. Netrin 1 mediates spinal cord oligodendrocyte precursor dispersal. *Development* **2003**, *130* (10), 2095-2105.

(45) Su, Y.; Wang, X.; Yang, Y.; Chen, L.; Xia, W.; Hoi, K. K.; Li, H.; Wang, Q.; Yu, G.; Chen, X.; et al. Astrocyte endfoot formation controls the termination of oligodendrocyte precursor cell perivascular migration during development. *Neuron* **2023**, *111* (2), 190-201.e198. DOI: 10.1016/j.neuron.2022.10.032.

(46) Fancy, S. P.; Baranzini, S. E.; Zhao, C.; Yuk, D. I.; Irvine, K. A.; Kaing, S.; Sanai, N.; Franklin, R. J.; Rowitch, D. H. Dysregulation of the Wnt pathway inhibits timely myelination and remyelination in the mammalian CNS. *Genes Dev* **2009**, *23* (13), 1571-1585. DOI: 10.1101/gad.1806309.

(47) Fancy, S. P.; Harrington, E. P.; Yuen, T. J.; Silbereis, J. C.; Zhao, C.; Baranzini, S. E.; Bruce, C. C.; Otero, J. J.; Huang, E. J.; Nusse, R.; et al. Axin2 as regulatory and therapeutic target in newborn brain injury and remyelination. *Nat Neurosci* **2011**, *14* (8), 1009-1016. DOI: 10.1038/nn.2855.

(48) Ortega, F.; Gascón, S.; Masserdotti, G.; Deshpande, A.; Simon, C.; Fischer, J.; Dimou, L.; Chichung Lie, D.; Schroeder, T.; Berninger, B. Oligodendrogliogenic and neurogenic adult subependymal zone neural stem cells constitute distinct lineages and exhibit differential responsiveness to Wnt signalling. *Nat Cell Biol* **2013**, *15* (6), 602-613. DOI: 10.1038/ncb2736.

(49) Fu, H.; Cai, J.; Clevers, H.; Fast, E.; Gray, S.; Greenberg, R.; Jain, M. K.; Ma, Q.; Qiu, M.; Rowitch, D. H.; et al. A genome-wide screen for spatially restricted expression patterns identifies transcription factors that regulate glial development. *J Neurosci* **2009**, *29* (36), 11399-11408. DOI: 10.1523/JNEUROSCI.0160-09.2009.

(50) Hughes, E. G.; Orthmann-Murphy, J. L.; Langseth, A. J.; Bergles, D. E. Myelin remodeling through experience-dependent oligodendrogenesis in the adult somatosensory cortex. *Nat Neurosci* **2018**, *21* (5), 696-706. DOI: 10.1038/s41593-018-0121-5.

(51) Fünfschilling, U.; Supplie, L. M.; Mahad, D.; Boretius, S.; Saab, A. S.; Edgar, J.; Brinkmann, B. G.; Kassmann, C. M.; Tzvetanova, I. D.; Möbius, W.; et al. Glycolytic oligodendrocytes maintain myelin and long-term axonal integrity. *Nature* **2012**, *485* (7399), 517-521. DOI: 10.1038/nature11007.

(52) Lee, S.; Chong, S. Y.; Tuck, S. J.; Corey, J. M.; Chan, J. R. A rapid and reproducible assay for modeling myelination by oligodendrocytes using engineered nanofibers. *Nat Protoc* **2013**, *8* (4), 771-782. DOI: 10.1038/nprot.2013.039.

(53) Yalçın, B.; Monje, M. Microenvironmental interactions of oligodendroglial cells. *Dev Cell* **2021**, *56* (13), 1821-1832. DOI: 10.1016/j.devcel.2021.06.006.

(54) McKenzie, I. A.; Ohayon, D.; Li, H.; de Faria, J. P.; Emery, B.; Tohyama, K.; Richardson, W. D. Motor skill learning requires active central myelination. *Science* **2014**, *346* (6207), 318-322. DOI: 10.1126/science.1254960.

(55) Swire, M.; Kotelevtsev, Y.; Webb, D. J.; Lyons, D. A.; Ffrench-Constant, C. Endothelin signalling mediates experience-dependent myelination in the CNS. *Elife* **2019**, *8*. DOI: 10.7554/eLife.49493.

(56) Osso, L. A.; Rankin, K. A.; Chan, J. R. Experience-dependent myelination following stress is mediated by the neuropeptide dynorphin. *Neuron* **2021**, *109* (22), 3619-3632.e3615. DOI: 10.1016/j.neuron.2021.08.015.

(57) Pan, S.; Mayoral, S. R.; Choi, H. S.; Chan, J. R.; Kheirbek, M. A. Preservation of a remote fear memory requires new myelin formation. *Nat Neurosci* **2020**, *23* (4), 487-499. DOI: 10.1038/s41593-019-0582-1.

(58) Louvi, A.; Grove, E. A. Cilia in the CNS: the quiet organelle claims center stage. *Neuron* **2011**, *69* (6), 1046-1060. DOI: 10.1016/j.neuron.2011.03.002.

(59) Anvarian, Z.; Mykytyn, K.; Mukhopadhyay, S.; Pedersen, L. B.; Christensen, S. T. Cellular signalling by primary cilia in development, organ function and disease. *Nat Rev Nephrol* **2019**, *15* (4), 199-219. DOI: 10.1038/s41581-019-0116-9.

(60) Reiter, J. F.; Leroux, M. R. Genes and molecular pathways underpinning ciliopathies. *Nat Rev Mol Cell Biol* **2017**, *18* (9), 533-547. DOI: 10.1038/nrm.2017.60.

(61) Seeley, E. S.; Nachury, M. V. The perennial organelle: assembly and disassembly of the primary cilium. *J Cell Sci* **2010**, *123* (Pt 4), 511-518. DOI: 10.1242/jcs.061093.

(62) Nigg, E. A.; Stearns, T. The centrosome cycle: Centriole biogenesis, duplication and inherent asymmetries. *Nat Cell Biol* **2011**, *13* (10), 1154-1160. DOI: 10.1038/ncb2345.

(63) Rosenbaum, J. L.; Witman, G. B. Intraflagellar transport. *Nat Rev Mol Cell Biol* **2002**, *3* (11), 813-825. DOI: 10.1038/nrm952.

(64) Follit, J. A.; Xu, F.; Keady, B. T.; Pazour, G. J. Characterization of mouse IFT complex B. *Cell Motil Cytoskeleton* **2009**, *66* (8), 457-468. DOI: 10.1002/cm.20346.

(65) Pedersen, L. B.; Rosenbaum, J. L. Intraflagellar transport (IFT) role in ciliary assembly, resorption and signalling. *Curr Top Dev Biol* **2008**, *85*, 23-61. DOI: 10.1016/S0070-2153(08)00802-8.

(66) Truong, M. E.; Bilekova, S.; Choksi, S. P.; Li, W.; Bugaj, L. J.; Xu, K.; Reiter, J. F. Vertebrate cells differentially interpret ciliary and extraciliary cAMP. *Cell* **2021**, *184* (11), 2911-2926.e2918. DOI: 10.1016/j.cell.2021.04.002.

(67) Corbit, K. C.; Aanstad, P.; Singla, V.; Norman, A. R.; Stainier, D. Y.; Reiter, J. F. Vertebrate Smoothened functions at the primary cilium. *Nature* **2005**, *437* (7061), 1018-1021. DOI: 10.1038/nature04117.

(68) Mukhopadhyay, S.; Wen, X.; Ratti, N.; Loktev, A.; Rangell, L.; Scales, S. J.; Jackson, P. K. The ciliary G-protein-coupled receptor Gpr161 negatively regulates the Sonic hedgehog pathway via cAMP signaling. *Cell* **2013**, *152* (1-2), 210-223. DOI: 10.1016/j.cell.2012.12.026.

(69) Mykytyn, K.; Askwith, C. G-Protein-Coupled Receptor Signaling in Cilia. *Cold Spring Harb Perspect Biol* **2017**, *9* (9). DOI: 10.1101/cshperspect.a028183.

(70) Briscoe, J.; Thérond, P. P. The mechanisms of Hedgehog signalling and its roles in development and disease. *Nat Rev Mol Cell Biol* **2013**, *14* (7), 416-429. DOI: 10.1038/nrm3598.

(71) Rowitch, D. H. Glial specification in the vertebrate neural tube. *Nat Rev Neurosci* **2004**, *5* (5), 409-419. DOI: 10.1038/nrn1389.

(72) Huangfu, D.; Liu, A.; Rakeman, A. S.; Murcia, N. S.; Niswander, L.; Anderson, K. V. Hedgehog signalling in the mouse requires intraflagellar transport proteins. *Nature* **2003**, *426* (6962), 83-87. DOI: 10.1038/nature02061.

(73) Rohatgi, R.; Milenkovic, L.; Scott, M. P. Patched1 regulates hedgehog signaling at the primary cilium. *Science* **2007**, *317* (5836), 372-376. DOI: 10.1126/science.1139740.

(74) Goetz, S. C.; Anderson, K. V. The primary cilium: a signalling centre during vertebrate development. *Nat Rev Genet* **2010**, *11* (5), 331-344. DOI: 10.1038/nrg2774.

(75) Lagerström, M. C.; Schiöth, H. B. Structural diversity of G protein-coupled receptors and significance for drug discovery. *Nat Rev Drug Discov* **2008**, *7* (4), 339-357. DOI: 10.1038/nrd2518.

(76) Schou, K. B.; Pedersen, L. B.; Christensen, S. T. Ins and outs of GPCR signaling in primary cilia. *EMBO Rep* **2015**, *16* (9), 1099-1113. DOI: 10.15252/embr.201540530.

(77) Händel, M.; Schulz, S.; Stanarius, A.; Schreff, M.; Erdtmann-Vourliotis, M.; Schmidt, H.; Wolf, G.; Höllt, V. Selective targeting of somatostatin receptor 3 to neuronal cilia. *Neuroscience* **1999**, *89* (3), 909-926. DOI: 10.1016/s0306-4522(98)00354-6.

(78) Einstein, E. B.; Patterson, C. A.; Hon, B. J.; Regan, K. A.; Reddi, J.; Melnikoff, D. E.; Mateer, M. J.; Schulz, S.; Johnson, B. N.; Tallent, M. K. Somatostatin signaling in neuronal cilia is critical for object recognition memory. *J Neurosci* **2010**, *30* (12), 4306-4314. DOI: 10.1523/JNEUROSCI.5295-09.2010.

(79) Siljee, J. E.; Wang, Y.; Bernard, A. A.; Ersoy, B. A.; Zhang, S.; Marley, A.; Von Zastrow, M.; Reiter, J. F.; Vaisse, C. Subcellular localization of MC4R with ADCY3 at neuronal primary cilia underlies a common pathway for genetic predisposition to obesity. *Nat Genet* **2018**, *50* (2), 180-185. DOI: 10.1038/s41588-017-0020-9.

(80) Wang, Y.; Bernard, A.; Comblain, F.; Yue, X.; Paillart, C.; Zhang, S.; Reiter, J. F.; Vaisse, C. Melanocortin 4 receptor signals at the neuronal primary cilium to control food intake and body weight. *J Clin Invest* **2021**, *131* (9). DOI: 10.1172/JCI142064.

(81) Loktev, A. V.; Jackson, P. K. Neuropeptide Y family receptors traffic via the Bardet-Biedl syndrome pathway to signal in neuronal primary cilia. *Cell Rep* **2013**, *5* (5), 1316-1329. DOI: 10.1016/j.celrep.2013.11.011.

(82) Koemeter-Cox, A. I.; Sherwood, T. W.; Green, J. A.; Steiner, R. A.; Berbari, N. F.; Yoder, B. K.; Kauffman, A. S.; Monsma, P. C.; Brown, A.; Askwith, C. C.; et al. Primary cilia enhance kisspeptin receptor signaling on gonadotropin-releasing hormone neurons. *Proc Natl Acad Sci U S A* **2014**, *111* (28), 10335-10340. DOI: 10.1073/pnas.1403286111.

(83) Berbari, N. F.; Johnson, A. D.; Lewis, J. S.; Askwith, C. C.; Mykytyn, K. Identification of ciliary localization sequences within the third intracellular loop of G protein-coupled receptors. *Mol Biol Cell* **2008**, *19* (4), 1540-1547. DOI: 10.1091/mbc.e07-09-0942.

(84) Brailov, I.; Bancila, M.; Brisorgueil, M. J.; Miquel, M. C.; Hamon, M.; Vergé, D. Localization of 5-HT(6) receptors at the plasma membrane of neuronal cilia in the rat brain. *Brain Res* **2000**, *872* (1-2), 271-275. DOI: 10.1016/s0006-8993(00)02519-1.

(85) Omori, Y.; Chaya, T.; Yoshida, S.; Irie, S.; Tsujii, T.; Furukawa, T. Identification of G Protein-Coupled Receptors (GPCRs) in Primary Cilia and Their Possible Involvement in Body Weight Control. *PLoS One* **2015**, *10* (6), e0128422. DOI: 10.1371/journal.pone.0128422.

(86) Spassky, N.; Han, Y. G.; Aguilar, A.; Strehl, L.; Besse, L.; Laclef, C.; Ros, M. R.; Garcia-Verdugo, J. M.; Alvarez-Buylla, A. Primary cilia are required for cerebellar development and Shh-dependent expansion of progenitor pool. *Dev Biol* **2008**, *317* (1), 246-259. DOI: 10.1016/j.ydbio.2008.02.026.

(87) Chizhikov, V. V.; Davenport, J.; Zhang, Q.; Shih, E. K.; Cabello, O. A.; Fuchs, J. L.; Yoder, B. K.; Millen, K. J. Cilia proteins control cerebellar morphogenesis by promoting expansion of the granule progenitor pool. *J Neurosci* **2007**, *27* (36), 9780-9789. DOI: 10.1523/JNEUROSCI.5586-06.2007.

(88) Tong, C. K.; Han, Y. G.; Shah, J. K.; Obernier, K.; Guinto, C. D.; Alvarez-Buylla, A. Primary cilia are required in a unique subpopulation of neural progenitors. *Proc Natl Acad Sci U S A* **2014**, *111* (34), 12438-12443. DOI: 10.1073/pnas.1321425111.

(89) Han, Y. G.; Spassky, N.; Romaguera-Ros, M.; Garcia-Verdugo, J. M.; Aguilar, A.; Schneider-Maunoury, S.; Alvarez-Buylla, A. Hedgehog signaling and primary cilia are required for the formation of adult neural stem cells. *Nat Neurosci* **2008**, *11* (3), 277-284. DOI: 10.1038/nn2059.

(90) Breunig, J. J.; Sarkisian, M. R.; Arellano, J. I.; Morozov, Y. M.; Ayoub, A. E.; Sojitra, S.; Wang, B.; Flavell, R. A.; Rakic, P.; Town, T. Primary cilia regulate hippocampal neurogenesis by mediating sonic hedgehog signaling. *Proc Natl Acad Sci U S A* **2008**, *105* (35), 13127-13132. DOI: 10.1073/pnas.0804558105.

(91) Higginbotham, H.; Eom, T. Y.; Mariani, L. E.; Bachleda, A.; Hirt, J.; Gukassyan, V.; Cusack, C. L.; Lai, C.; Caspary, T.; Anton, E. S. Arl13b in primary cilia regulates the migration and placement of interneurons in the developing cerebral cortex. *Dev Cell* **2012**, *23* (5), 925-938. DOI: 10.1016/j.devcel.2012.09.019.

(92) Falcón-Urrutia, P.; Carrasco, C. M.; Lois, P.; Palma, V.; Roth, A. D. Shh Signaling through the Primary Cilium Modulates Rat Oligodendrocyte Differentiation. *PLoS One* **2015**, *10* (7), e0133567. DOI: 10.1371/journal.pone.0133567.

(93) Cullen, C. L.; O'Rourke, M.; Beasley, S. J.; Auderset, L.; Zhen, Y.; Pepper, R. E.; Gasperini, R.; Young, K. M. Kif3a deletion prevents primary cilia assembly on oligodendrocyte progenitor cells, reduces oligodendrogenesis and impairs fine motor function. *Glia* **2021**, *69* (5), 1184-1203. DOI: 10.1002/glia.23957.

(94) Delfino, G.; Bénardais, K.; Graff, J.; Samama, B.; Antal, M. C.; Ghandour, M. S.; Boehm, N. Oligodendroglial primary cilium heterogeneity during development and demyelination/remyelination. *Front Cell Neurosci* **2022**, *16*, 1049468. DOI: 10.3389/fncel.2022.1049468.

(95) Wang, L. C.; Almazan, G. Role of Sonic Hedgehog Signaling in Oligodendrocyte Differentiation. *Neurochem Res* **2016**, *41* (12), 3289-3299. DOI: 10.1007/s11064-016-2061-3.

(96) Xu, X.; Yu, Q.; Fang, M.; Yi, M.; Yang, A.; Xie, B.; Yang, J.; Zhang, Z.; Dai, Z.; Qiu, M. Stage-specific regulation of oligodendrocyte development by Hedgehog signaling in the spinal cord. *Glia* **2020**, *68* (2), 422-434. DOI: 10.1002/glia.23729.

(97) Loulier, K.; Ruat, M.; Traiffort, E. Increase of proliferating oligodendroglial progenitors in the adult mouse brain upon Sonic hedgehog delivery in the lateral ventricle. *J Neurochem* **2006**, *98* (2), 530-542. DOI: 10.1111/j.1471-4159.2006.03896.x.

(98) Ferent, J.; Zimmer, C.; Durbec, P.; Ruat, M.; Traiffort, E. Sonic Hedgehog signaling is a positive oligodendrocyte regulator during demyelination. *J Neurosci* **2013**, *33* (5), 1759-1772. DOI: 10.1523/JNEUROSCI.3334-12.2013.

(99) Lein, E. S.; Hawrylycz, M. J.; Ao, N.; Ayres, M.; Bensinger, A.; Bernard, A.; Boe, A. F.; Boguski, M. S.; Brockway, K. S.; Byrnes, E. J.; et al. Genome-wide atlas of gene expression in the adult mouse brain. *Nature* **2007**, *445* (7124), 168-176. DOI: 10.1038/nature05453.

(100) Ackerman, S. D.; Garcia, C.; Piao, X.; Gutmann, D. H.; Monk, K. R. The adhesion GPCR Gpr56 regulates oligodendrocyte development via interactions with Gα12/13 and RhoA. *Nat Commun* **2015**, *6*, 6122. DOI: 10.1038/ncomms7122.

(101) Giera, S.; Deng, Y.; Luo, R.; Ackerman, S. D.; Mogha, A.; Monk, K. R.; Ying, Y.; Jeong, S. J.; Makinodan, M.; Bialas, A. R.; et al. The adhesion G protein-coupled receptor GPR56 is a cell-autonomous regulator of oligodendrocyte development. *Nat Commun* **2015**, *6*, 6121. DOI: 10.1038/ncomms7121.

(102) Chen, Y.; Wu, H.; Wang, S.; Koito, H.; Li, J.; Ye, F.; Hoang, J.; Escobar, S. S.; Gow, A.; Arnett, H. A.; et al. The oligodendrocyte-specific G protein-coupled receptor GPR17 is a

cell-intrinsic timer of myelination. *Nat Neurosci* **2009**, *12* (11), 1398-1406. DOI: 10.1038/nn.2410.

(103) Lu, C.; Dong, L.; Zhou, H.; Li, Q.; Huang, G.; Bai, S. J.; Liao, L. G-Protein-Coupled Receptor Gpr17 Regulates Oligodendrocyte Differentiation in Response to Lysolecithin-Induced Demyelination. *Sci Rep* **2018**, *8* (1), 4502. DOI: 10.1038/s41598-018-22452-0.

(104) Yang, H. J.; Vainshtein, A.; Maik-Rachline, G.; Peles, E. G protein-coupled receptor 37 is a negative regulator of oligodendrocyte differentiation and myelination. *Nat Commun* **2016**, *7*, 10884. DOI: 10.1038/ncomms10884.

(105) Franklin, R. J. M.; Ffrench-Constant, C. Regenerating CNS myelin - from mechanisms to experimental medicines. *Nat Rev Neurosci* **2017**, *18* (12), 753-769. DOI: 10.1038/nrn.2017.136.

(106) Mick, D. U.; Rodrigues, R. B.; Leib, R. D.; Adams, C. M.; Chien, A. S.; Gygi, S. P.; Nachury, M. V. Proteomics of Primary Cilia by Proximity Labeling. *Dev Cell* **2015**, *35* (4), 497-512. DOI: 10.1016/j.devcel.2015.10.015.

(107) May, E. A.; Kalocsay, M.; D'Auriac, I. G.; Schuster, P. S.; Gygi, S. P.; Nachury, M. V.; Mick, D. U. Time-resolved proteomics profiling of the ciliary Hedgehog response. *J Cell Biol* **2021**, *220* (5). DOI: 10.1083/jcb.202007207.

(108) Ishikawa, H.; Thompson, J.; Yates, J. R.; Marshall, W. F. Proteomic analysis of mammalian primary cilia. *Curr Biol* **2012**, *22* (5), 414-419. DOI: 10.1016/j.cub.2012.01.031.

(109) Fancy, S. P.; Chan, J. R.; Baranzini, S. E.; Franklin, R. J.; Rowitch, D. H. Myelin regeneration: a recapitulation of development? *Annu Rev Neurosci* **2011**, *34*, 21-43. DOI: 10.1146/annurev-neuro-061010-113629.

(110) Gallo, V.; Deneen, B. Glial development: the crossroads of regeneration and repair in the CNS. *Neuron* **2014**, *83* (2), 283-308. DOI: 10.1016/j.neuron.2014.06.010.

(111) Bradl, M.; Lassmann, H. Oligodendrocytes: biology and pathology. *Acta Neuropathol* **2010**, *119* (1), 37-53. DOI: 10.1007/s00401-009-0601-5.

(112) Elbaz, B.; Popko, B. Molecular Control of Oligodendrocyte Development. *Trends Neurosci* **2019**, *42* (4), 263-277. DOI: 10.1016/j.tins.2019.01.002.

(113) Hughes, E. G.; Kang, S. H.; Fukaya, M.; Bergles, D. E. Oligodendrocyte progenitors balance growth with self-repulsion to achieve homeostasis in the adult brain. *Nat Neurosci* **2013**, *16* (6), 668-676. DOI: 10.1038/nn.3390.

(114) Singla, V.; Reiter, J. F. The primary cilium as the cell's antenna: signaling at a sensory organelle. *Science* **2006**, *313* (5787), 629-633. DOI: 10.1126/science.1124534.

(115) Gigante, E. D.; Caspary, T. Signaling in the primary cilium through the lens of the Hedgehog pathway. *Wiley Interdiscip Rev Dev Biol* **2020**, *9* (6), e377. DOI: 10.1002/wdev.377.

(116) May, S. R.; Ashique, A. M.; Karlen, M.; Wang, B.; Shen, Y.; Zarbalis, K.; Reiter, J.; Ericson, J.; Peterson, A. S. Loss of the retrograde motor for IFT disrupts localization of Smo to cilia and prevents the expression of both activator and repressor functions of Gli. *Dev Biol* **2005**, *287* (2), 378-389. DOI: 10.1016/j.ydbio.2005.08.050.

(117) Merchán, P.; Bribián, A.; Sánchez-Camacho, C.; Lezameta, M.; Bovolenta, P.; de Castro, F. Sonic hedgehog promotes the migration and proliferation of optic nerve oligodendrocyte precursors. *Mol Cell Neurosci* **2007**, *36* (3), 355-368. DOI: 10.1016/j.mcn.2007.07.012.

(118) Komorowska, K.; Doyle, A.; Wahlestedt, M.; Subramaniam, A.; Debnath, S.; Chen, J.; Soneji, S.; Van Handel, B.; Mikkola, H. K. A.; Miharada, K.; et al. Hepatic Leukemia Factor Maintains Quiescence of Hematopoietic Stem Cells and Protects the Stem Cell Pool during Regeneration. *Cell Rep* **2017**, *21* (12), 3514-3523. DOI: 10.1016/j.celrep.2017.11.084.

(119) Pullamsetti, S. S.; Banat, G. A.; Schmall, A.; Szibor, M.; Pomagruk, D.; Hänze, J.; Kolosionek, E.; Wilhelm, J.; Braun, T.; Grimminger, F.; et al. Phosphodiesterase-4 promotes proliferation and angiogenesis of lung cancer by crosstalk with HIF. *Oncogene* **2013**, *32* (9), 1121-1134. DOI: 10.1038/onc.2012.136.

(120) Xie, W.; Miehe, M.; Laufer, S.; Johnsen, S. A. The H2B ubiquitin-protein ligase RNF40 is required for somatic cell reprogramming. *Cell Death Dis* **2020**, *11* (4), 287. DOI: 10.1038/s41419-020-2482-4.

(121) Cubillos-Rojas, M.; Schneider, T.; Hadjebi, O.; Pedrazza, L.; de Oliveira, J. R.; Langa, F.; Guénet, J. L.; Duran, J.; de Anta, J. M.; Alcántara, S.; et al. The HERC2 ubiquitin ligase is essential for embryonic development and regulates motor coordination. *Oncotarget* **2016**, *7* (35), 56083-56106. DOI: 10.18632/oncotarget.11270.

(122) Fang, C.; Chen, Y. X.; Wu, N. Y.; Yin, J. Y.; Li, X. P.; Huang, H. S.; Zhang, W.; Zhou, H. H.; Liu, Z. Q. MiR-488 inhibits proliferation and cisplatin sensibility in non-small-cell lung cancer (NSCLC) cells by activating the eIF3a-mediated NER signaling pathway. *Sci Rep* **2017**, *7*, 40384. DOI: 10.1038/srep40384.

(123) Cervantes, S.; Fontcuberta-PiSunyer, M.; Servitja, J. M.; Fernandez-Ruiz, R.; García, A.; Sanchez, L.; Lee, Y. S.; Gomis, R.; Gasa, R. Late-stage differentiation of embryonic pancreatic β-cells requires Jarid2. *Sci Rep* **2017**, *7* (1), 11643. DOI: 10.1038/s41598-017-11691-2.

(124) Miyatsuka, T.; Kosaka, Y.; Kim, H.; German, M. S. Neurogenin3 inhibits proliferation in endocrine progenitors by inducing Cdkn1a. *Proc Natl Acad Sci U S A* **2011**, *108* (1), 185-190. DOI: 10.1073/pnas.1004842108.

(125) Ding, B. S.; Nolan, D. J.; Butler, J. M.; James, D.; Babazadeh, A. O.; Rosenwaks, Z.; Mittal, V.; Kobayashi, H.; Shido, K.; Lyden, D.; et al. Inductive angiocrine signals from sinusoidal endothelium are required for liver regeneration. *Nature* **2010**, *468* (7321), 310-315. DOI: 10.1038/nature09493.

(126) Shaywitz, A. J.; Greenberg, M. E. CREB: a stimulus-induced transcription factor activated by a diverse array of extracellular signals. *Annu Rev Biochem* **1999**, *68*, 821-861. DOI: 10.1146/annurev.biochem.68.1.821.

(127) Xie, F.; Li, B. X.; Kassenbrock, A.; Xue, C.; Wang, X.; Qian, D. Z.; Sears, R. C.; Xiao, X. Identification of a Potent Inhibitor of CREB-Mediated Gene Transcription with Efficacious in Vivo Anticancer Activity. *J Med Chem* **2015**, *58* (12), 5075-5087. DOI: 10.1021/acs.jmedchem.5b00468.

(128) Messersmith, D. J.; Murtie, J. C.; Le, T. Q.; Frost, E. E.; Armstrong, R. C. Fibroblast growth factor 2 (FGF2) and FGF receptor expression in an experimental demyelinating disease with extensive remyelination. *J Neurosci Res* **2000**, *62* (2), 241-256. DOI: 10.1002/1097-4547(20001015)62:2<241::AID-JNR9>3.0.CO;2-D.

(129) Scafidi, J.; Hammond, T. R.; Scafidi, S.; Ritter, J.; Jablonska, B.; Roncal, M.; Szigeti-Buck, K.; Coman, D.; Huang, Y.; McCarter, R. J.; et al. Intranasal epidermal growth factor treatment rescues neonatal brain injury. *Nature* **2014**, *506* (7487), 230-234. DOI: 10.1038/nature12880.

(130) Spassky, N.; Heydon, K.; Mangatal, A.; Jankovski, A.; Olivier, C.; Queraud-Lesaux, F.; Goujet-Zalc, C.; Thomas, J. L.; Zalc, B. Sonic hedgehog-dependent emergence of oligodendrocytes in the telencephalon: evidence for a source of oligodendrocytes in the olfactory bulb that is independent of PDGFRalpha signaling. *Development* **2001**, *128* (24), 4993-5004. DOI: 10.1242/dev.128.24.4993.

(131) Fan, C. W.; Chen, B.; Franco, I.; Lu, J.; Shi, H.; Wei, S.; Wang, C.; Wu, X.; Tang, W.; Roth, M. G.; et al. The Hedgehog pathway effector smoothened exhibits signaling competency in the absence of ciliary accumulation. *Chem Biol* **2014**, *21* (12), 1680-1689. DOI: 10.1016/j.chembiol.2014.10.013.

(132) Lee, M. M.; Badache, A.; DeVries, G. H. Phosphorylation of CREB in axon-induced Schwann cell proliferation. *J Neurosci Res* **1999**, *55* (6), 702-712. DOI: 10.1002/(SICI)1097-4547(19990315)55:6<702::AID-JNR5>3.0.CO;2-N.

(133) Long, F.; Schipani, E.; Asahara, H.; Kronenberg, H.; Montminy, M. The CREB family of activators is required for endochondral bone development. *Development* **2001**, *128* (4), 541-550. DOI: 10.1242/dev.128.4.541.

(134) Johnson, J. R.; Chu, A. K.; Sato-Bigbee, C. Possible role of CREB in the stimulation of oligodendrocyte precursor cell proliferation by neurotrophin-3. *J Neurochem* **2000**, *74* (4), 1409-1417. DOI: 10.1046/j.1471-4159.2000.0741409.x.

(135) Adams, K. L.; Dahl, K. D.; Gallo, V.; Macklin, W. B. Intrinsic and extrinsic regulators of oligodendrocyte progenitor proliferation and differentiation. *Semin Cell Dev Biol* **2021**, *116*, 16-24. DOI: 10.1016/j.semcdb.2020.10.002.

(136) Gonçalves, J.; Pelletier, L. The Ciliary Transition Zone: Finding the Pieces and Assembling the Gate. *Mol Cells* **2017**, *40* (4), 243-253. DOI: 10.14348/molcells.2017.0054.

(137) Brewer, K. M.; Engle, S. E.; Bansal, R.; Brewer, K. K.; Jasso, K. R.; McIntyre, J. C.; Vaisse, C.; Reiter, J. F.; Berbari, N. F. Physiological Condition-Dependent Changes in Ciliary GPCR Localization in the Brain. *eNeuro* **2023**, *10* (3). DOI: 10.1523/ENEURO.0360-22.2023.

(138) Wiegering, A.; Dildrop, R.; Kalfhues, L.; Spychala, A.; Kuschel, S.; Lier, J. M.; Zobel, T.; Dahmen, S.; Leu, T.; Struchtrup, A.; et al. Cell type-specific regulation of ciliary transition zone assembly in vertebrates. *EMBO J* **2018**, *37* (10). DOI: 10.15252/embj.201797791.

(139) Kucharova, K.; Chang, Y.; Boor, A.; Yong, V. W.; Stallcup, W. B. Reduced inflammation accompanies diminished myelin damage and repair in the NG2 null mouse spinal cord. *J Neuroinflammation* **2011**, *8*, 158. DOI: 10.1186/1742-2094-8-158.

(140) Ventura, A.; Meissner, A.; Dillon, C. P.; McManus, M.; Sharp, P. A.; Van Parijs, L.; Jaenisch, R.; Jacks, T. Cre-lox-regulated conditional RNA interference from transgenes. *Proc Natl Acad Sci U S A* **2004**, *101* (28), 10380-10385. DOI: 10.1073/pnas.0403954101.

(141) Dobin, A.; Davis, C. A.; Schlesinger, F.; Drenkow, J.; Zaleski, C.; Jha, S.; Batut, P.; Chaisson, M.; Gingeras, T. R. STAR: ultrafast universal RNA-seq aligner. *Bioinformatics* **2013**, *29* (1), 15-21. DOI: 10.1093/bioinformatics/bts635.

(142) Love, M. I.; Huber, W.; Anders, S. Moderated estimation of fold change and dispersion for RNA-seq data with DESeq2. *Genome Biol* **2014**, *15* (12), 550. DOI: 10.1186/s13059-014-0550-8.

(143) Roesch, K.; Jadhav, A. P.; Trimarchi, J. M.; Stadler, M. B.; Roska, B.; Sun, B. B.; Cepko, C. L. The transcriptome of retinal Müller glial cells. *J Comp Neurol* **2008**, *509* (2), 225-238. DOI: 10.1002/cne.21730.

(144) Kang, S. H.; Fukaya, M.; Yang, J. K.; Rothstein, J. D.; Bergles, D. E. NG2+ CNS glial progenitors remain committed to the oligodendrocyte lineage in postnatal life and following neurodegeneration. *Neuron* **2010**, *68* (4), 668-681. DOI: 10.1016/j.neuron.2010.09.009.

(145) Srinivas, S.; Watanabe, T.; Lin, C. S.; William, C. M.; Tanabe, Y.; Jessell, T. M.; Costantini, F. Cre reporter strains produced by targeted insertion of EYFP and ECFP into the ROSA26 locus. *BMC Dev Biol* **2001**, *1*, 4. DOI: 10.1186/1471-213x-1-4.

(146) Haycraft, C. J.; Zhang, Q.; Song, B.; Jackson, W. S.; Detloff, P. J.; Serra, R.; Yoder, B. K. Intraflagellar transport is essential for endochondral bone formation. *Development* **2007**, *134* (2), 307-316. DOI: 10.1242/dev.02732.

(147) Lobingier, B. T.; Hüttenhain, R.; Eichel, K.; Miller, K. B.; Ting, A. Y.; von Zastrow, M.; Krogan, N. J. An Approach to Spatiotemporally Resolve Protein Interaction Networks in Living Cells. *Cell* **2017**, *169* (2), 350-360.e312. DOI: 10.1016/j.cell.2017.03.022.

Publishing Agreement

It is the policy of the University to encourage open access and broad distribution of all theses, dissertations, and manuscripts. The Graduate Division will facilitate the distribution of UCSF theses, dissertations, and manuscripts to the UCSF Library for open access and distribution. UCSF will make such theses, dissertations, and manuscripts accessible to the public and will take reasonable steps to preserve these works in perpetuity.

I hereby grant the non-exclusive, perpetual right to The Regents of the University of California to reproduce, publicly display, distribute, preserve, and publish copies of my thesis, dissertation, or manuscript in any form or media, now existing or later derived, including access online for teaching, research, and public service purposes.

_____   5/1/2023
Author Signature   Date